Pollen tube-triggered accumulation of NORTIA at the filiform apparatus facilitates fertilization in *Arabidopsis thaliana*

Jing Yuan[1,2*], Yan Ju[1,2*], Daniel S. Jones[4,5], Weiwei Zhang[2,3], Noel Lucca[1,2], Christopher J. Staiger[1,2,3], and Sharon A. Kessler[1,2,**]

[1]Department of Botany and Plant Pathology, Purdue University, West Lafayette, Indiana USA
[2]Purdue Center for Plant Biology, Purdue University, West Lafayette, Indiana USA
[3]Department of Biological Sciences, Purdue University, West Lafayette, Indiana USA
[4]Biology Department, The University of North Carolina at Chapel Hill, Chapel Hill, North Carolina USA (current address)
[5]Department of Microbiology and Plant Biology, University of Oklahoma, Norman, Oklahoma USA
*These authors contributed equally

** Corresponding author
Email: sakessler@purdue.edu

Abstract

During gamete delivery in *Arabidopsis thaliana*, intercellular communication between the attracted pollen tube and the receptive synergid cell leads to subcellular events in both cells culminating in the rupture of the tip-growing pollen tube and release of the sperm cells to achieve double fertilization. Live imaging of pollen tube reception revealed dynamic subcellular changes that occur in the female synergid cells. Pollen tube arrival triggers the trafficking of NORTIA (NTA) MLO protein from Golgi-associated compartments and the accumulation of endosomes at or near the synergid filiform apparatus, a membrane-rich region that acts as the site of communication between the pollen tube and synergids. Domain swaps and site-directed mutagenesis reveal that NTA's C-terminal cytoplasmic tail with its calmodulin-binding domain influences the subcellular localization and function of NTA in pollen tube reception and that early

accumulation of NTA at the filiform apparatus is sufficient for MLO function in pollen tube reception.

Key words

MLO, Pollination, gametophyte, synergid, pollen tube reception, calmodulin binding domain

Introduction

Intercellular communication is central to the proper development and maintenance of all multicellular organisms. During this communication, signals from one cell are perceived by receptors in another cell and translated into various subcellular responses. These responses include signal transduction cascades leading to transcription of other genes, calcium signaling, and trafficking of proteins to different organelles or regions of the cell. A well-studied example of signal-induced protein trafficking in plant development is the redistribution of the PIN polar auxin transporters to different sides of the cell during important developmental events such as embryo patterning, leaf initiation and lateral root initiation (Petrasek et al., 2006; Naramoto, 2017; Salanenka et al., 2018). In plants, most intercellular communication occurs between cells that are genetically identical and connected by adjoining cell walls. One exception is pollination, in which pollen (the male gametophyte) is released from an anther, transported to a receptive stigma, and produces a tip-growing pollen tube that grows through the female tissues of the pistil and delivers the two sperm cells to the female gametophyte (also known as the embryo sac, Figure 1A). The pollen tube's journey through the pistil requires cell-to-cell interactions with the female that allows water and nutrient uptake and enables the detection of cues important for guidance toward the female gametes (Johnson et al., 2019).

In the model plant *Arabidopsis thaliana*, complex signaling events ranging from pollen landing on the stigma to fusion of gametes occur over several hours. Most of our knowledge about the signaling pathways involved along the pollen tube's journey through the female is limited to the

56 final stages of pollination and involve a highly specialized pair of female gametophyte cells
57 known as synergids. During female gametophyte development, meiosis followed by three
58 rounds of mitosis produce the egg cell and central cell along with 2 synergid cells flanking the
59 egg cell and 3 antipodal cells on the chalazal end of the embryo sac (Drews and Yadegari,
60 2002), Figure 1A). The synergid cells are accessory cells that control the behavior of the pollen
61 tube during the final stages of pollination. Before pollen tube arrival, they secrete cysteine-rich
62 LURE peptides that act as short-range pollen tube attractants that are recognized by receptor-
63 like kinases in the tip of the pollen tube to regulate the direction of pollen tube growth and guide
64 the pollen tube to the micropyle of the ovule (Okuda et al., 2009; Takeuchi and Higashiyama,
65 2016; Wang et al., 2016). After pollen tube arrival, the synergids communicate with the pollen
66 tube to induce changes that result in pollen tube rupture and delivery of the sperm cells (Kessler
67 and Grossniklaus, 2011; Johnson et al., 2019). Thus, synergids are critical for ensuring that
68 double fertilization can occur to produce seeds.
69
70 In Arabidopsis, live imaging has been used to examine the behavior of both the pollen tube and
71 the synergids during the process of pollen tube reception. A pollen tube follows the gradient of
72 LURE attractants, enters the micropyle of the ovule, and pauses its growth for 30 min to 1 h just
73 outside the receptive synergid (Iwano et al., 2012; Denninger et al., 2014; Ngo et al., 2014).
74 During this pause in pollen tube growth, communication occurs between the pollen tube and the
75 synergids leading to subcellular changes and ultimately the death of both the pollen tube and
76 the receptive synergid. Cytoplasmic calcium oscillations occur in both the tip of the pollen tube
77 and in the 2 synergid cells during this communication phase. Cytoplasmic calcium levels
78 continue to increase in both cell types until the pollen tube starts to grow again and bursts to
79 release the sperm cells, a catastrophic event for both the pollen tube and the receptive
80 synergid, which also degenerates (Iwano et al., 2012; Denninger et al., 2014; Ngo et al., 2014).
81 Mutations in genes that regulate communication between the synergids and pollen tube during

82 pollen tube reception result in a pollen tube overgrowth phenotype in which the pollen tubes are
83 attracted normally to the ovules, but do not get the signal to burst and release the sperm cells.
84 Presumably, synergid-induced changes in the cell wall of the pollen tube tip do not occur in
85 these mutants, therefore the pollen tube continues to grow and coil inside the embryo sac.
86 Synergid-expressed genes that participate in pollen tube reception include the FERONIA (FER)
87 receptor-like kinase, the GPI-anchored protein LORELEI (LRE), and the Mildew Resistance
88 Locus-O (MLO) protein NORTIA (NTA, also known as AtMLO7) (Escobar-Restrepo et al., 2007;
89 Capron et al., 2008; Kessler et al., 2010; Ngo et al., 2014; Li et al., 2015; Liu et al., 2016).
90 Mutations in all of these genes lead to the pollen tube overgrowth phenotype due to disruption
91 of the pollen tube-synergid communication pathway.
92
93 FER and LRE are necessary for the calcium oscillations that occur in synergids in response to
94 pollen tube arrival (Ngo et al., 2014). In contrast, *nta-1* mutants have $[Ca^{2+}]_{cyto}$ oscillations at
95 lower amplitudes, indicating that NTA may participate in modulating Ca^{2+} fluxes in the synergids
96 during communication with the pollen tube and likely acts downstream of FER and LRE (Ngo et
97 al., 2014). Like all members of the MLO gene family, NTA has seven membrane-spanning
98 domains and a predicted calmodulin-binding domain (CaMBD) in its C-terminal intracellular tail
99 (Devoto et al., 2003; Kusch et al., 2016). Calmodulin (CaM) is a small protein that binds Ca^{2+}
100 and is involved in signal transduction for many cellular processes (Yang and Poovaiah, 2003).
101 We previously showed that the C-terminal domain of NTA could confer pollen tube reception
102 function to the related MLO8 protein (Jones et al., 2017), but the significance of the CaMBD in
103 pollen tube reception remains an open question.
104
105 The subcellular localization of these important pollen tube reception proteins is not always
106 predictive of their function in communicating with the pollen tube. As expected for early
107 response proteins, both FER and LRE are expressed in synergid cells where they localize in or

108 near a specialized region called the filiform apparatus, a membrane rich area located at the
109 micropyle end of the synergids (Huck et al., 2003; Rotman et al., 2003; Escobar-Restrepo et al.,
110 2007; Capron et al., 2008; Li et al., 2015; Lindner et al., 2015; Liu et al., 2016). The filiform
111 apparatus is thought to be important for the secretion of attractant peptides and is the first site of
112 interaction between the pollen tube and synergid cell prior to pollen tube reception (Mansfield et
113 al., 1991; Huang and Russell, 1992; Leshem et al., 2013). In contrast, before pollen tube arrival,
114 NTA is localized to a Golgi-associated compartment within the synergid cell and absent from the
115 filiform apparatus (Jones et al., 2017). At the end of pollen tube reception, NTA protein is only
116 detected at the filiform apparatus, indicating that this protein changes its subcellular localization
117 during pollen tube reception (Kessler et al., 2010). This suggests that pollen tube-triggered
118 regulation of the synergid secretory system may be a crucial subcellular response to pollen tube
119 arrival and that NTA function may be related to its subcellular distribution; however, the precise
120 timing and significance of NTA's redistribution remain unclear.
121
122 Here, we use a live-imaging system to further characterize synergid cellular dynamics during
123 pollen tube reception and to determine the timing and significance of the polar redistribution of
124 NTA to the filiform apparatus. To investigate the link between Ca^{2+} and MLO function in pollen
125 tube reception, we assayed the influence of the CaMBD on NTA's function and subcellular
126 distribution through C-terminal truncations and a point mutation disrupting the CaMBD. We
127 show that the polar redistribution of NTA is triggered by the approach of a pollen tube, is
128 important for pollen tube reception, and is facilitated by the CaMBD. While most subcellular
129 compartments remain distributed throughout the synergid cells during pollen tube reception,
130 recycling endosomes respond to pollen tube arrival by accumulating towards the filiform
131 apparatus. Moreover, we show that targeting NTA to the filiform apparatus before pollen tube
132 attraction does not induce synergid cell death.
133

134 **Results**

135 **NORTIA Dynamically Redistributes to the Filiform Apparatus during Pollen Tube**

136 **Reception**

137 Pollen tube reception requires synergid cells to recognize the approaching pollen tube and to
138 send signals back to the pollen tube that result in release of the sperm cells at the correct time
139 and place so that double fertilization can be completed. Based on static images, we previously
140 reported that NTA-GFP fusion protein localizes to a Golgi-associated compartment in synergids
141 prior to pollen tube attraction (Jones et al., 2017). When imaged after pollen tube reception,
142 NTA-GFP is concentrated at the micropylar end of the synergid (in or near the filiform
143 apparatus) (Kessler et al., 2010). NTA-GFP does not accumulate at the filiform apparatus in *fer*
144 ovules with pollen tube overgrowth, suggesting that FER-mediated signaling during pollen tube
145 reception triggers NTA-GFP redistribution that in turn contributes to the interaction of the
146 synergid with the pollen tube (Kessler et al., 2010). An alternative hypothesis is that pollen tube
147 rupture triggers NTA-GFP redistribution and is a symptom of pollen tube reception rather than
148 an important contributor to the signaling pathway. To distinguish between these two
149 possibilities, we used a semi-*in vivo* pollination system combined with time-lapse spinning disk
150 confocal microscopy to determine the timing of NTA-GFP redistribution during the pollen tube
151 reception process. In the semi-*in vivo* system, pollen tubes grow out of a cut style and are
152 attracted to ovules arranged on pollen germination media (Palanivelu and Preuss, 2006). This
153 system has previously been used to quantify and track pollen tube attraction to ovules and to
154 image $[Ca^{2+}]_{cyto}$ reporters during pollen tube reception (Hamamura et al., 2011; Hamamura et
155 al., 2012; Denninger et al., 2014; Hamamura et al., 2014; Ngo et al., 2014).

156

157 To follow subcellular changes in NTA-GFP protein localization before, during, and after pollen
158 tube arrival, we used pollen from plants expressing the pollen-specific *AUTOINHIBITED* Ca^{2+}-
159 *ATPase9*$_{pro}$*::DsRed* (*ACA9*$_{pro}$*::DsRed*) reporter and ovules expressing *NTA*$_{pro}$*::NTA-GFP* in the

160 semi-*in vivo* system. Approximately 4 h after pollination, pollen tubes emerged from the style
161 onto the media and were attracted to ovules (Figure 1B). Fluorescence images in both channels
162 were collected every 5 min from when a pollen tube approached an ovule until after the pollen
163 tube ruptured inside the ovule. In ~83% (n=93) of the ovules that attracted a pollen tube and
164 successfully burst to deliver the sperm cells, NTA-GFP accumulated at the filiform apparatus of
165 the synergids (Figures 1C-E). The rest of the ovules (~17%) attracted pollen tubes that stopped
166 growing in the micropyle and did not rupture. In these ovules, NTA-GFP did not accumulate in
167 the filiform apparatus. To exclude the possibility that prolonged imaging causes stress in
168 synergids which leads to filiform apparatus accumulation of NTA-GFP, we analyzed neighboring
169 ovules that did not attract pollen tubes but were imaged together with ovules that attracted
170 pollen tubes. NTA-GFP did not accumulate at the filiform apparatus in these ovules (n=103)
171 (Figure 1F). Likewise, ovules that were incubated on pollen germination media without a
172 pollinated pistil (n=133, Figures 1F and S1) and imaged over the same time frame did not
173 accumulate NTA-GFP in the filiform apparatus. These data indicate that pollen tube arrival is
174 necessary for NTA-GFP accumulation at the filiform apparatus rather than being retained in the
175 Golgi, and that this accumulation is not an artifact of the semi- *in vivo* imaging system. (Figure
176 1F).
177
178 Our semi-*in vivo* system also allowed us to determine the timing of NTA-GFP accumulation at
179 the filiform apparatus in relation to the position of the pollen tube as it approached the
180 synergids. We defined the 0 min timepoint as the time where the pollen tube just reached the
181 micropylar opening of the ovule (Figure 1C, ovules with yellow stars, Movies S1 and S2). In all
182 cases, the shift of NTA-GFP signal from the Golgi to the filiform apparatus also started from this
183 time point. During the following 30–50 min, pollen tubes grew through the micropyle region of
184 ovule and arrived at the filiform apparatus of the receptive synergid cell. During this time, three
185 quarters to half of the NTA-GFP signal moved to the micropylar end of synergid cells, indicating

186 that the approach of the pollen tube triggers NTA-GFP accumulation at the filiform apparatus.
187 As reported in Ngo et al., 2014 and Denninger et al., 2014, the arriving pollen tubes paused
188 their growth outside the filiform apparatus for 30–50 min, presumably for cell-to-cell
189 communication. During this period, the NTA-GFP signal continued to shift toward the filiform
190 apparatus. At 70–80 min after pollen tube arrival at the micropyle, NTA-GFP signal was only
191 detected in the filiform apparatus and pollen tubes resumed growth and ruptured to release the
192 sperm cells (Figures 1C, D and Movies S1 and S2). Even though only one of the synergids
193 receives the pollen tube, NTA-GFP accumulated at the filiform apparatus in both synergid cells
194 in response to pollen tube arrival, similar to the activation of $[Ca^{2+}]_{cyto}$ oscillations in both
195 synergids during pollen tube reception reported in (Ngo et al., 2014).
196
197 **Golgi do not concentrate at the filiform apparatus during pollen tube reception**
198 We previously determined that NTA is sequestered in a Golgi-associated compartment in
199 synergid cells that have not attracted a pollen tube (Jones et al., 2017) . Our live-imaging data
200 suggest that NTA-GFP is selectively moved out of the Golgi and transported to the filiform
201 apparatus in response to pollen tube arrival; however, it is possible that the observed NTA-GFP
202 accumulation at the filiform apparatus is a result of massive reorganization of subcellular
203 compartments. To distinguish between these possibilities, we investigated the behavior of Golgi
204 in synergid cells during pollen tube reception. We used the semi-*in vivo* imaging system
205 described above with a synergid-expressed Golgi marker (Man49-mCherry) co-expressed with
206 NTA-GFP (Jones et al., 2018). In all replicates, the Golgi marker was distributed throughout the
207 synergids, excluded from the filiform apparatus, and co-localized with NTA-GFP as reported
208 previously (Figure 2A, n=93). When a pollen tube approached the synergids, NTA-GFP
209 accumulated at the filiform apparatus region of the synergids as observed previously (Figure 1),
210 but the Golgi-mCherry marker remained consistently distributed throughout the synergid cells
211 and did not concentrate near the filiform apparatus (Figure 2B). In order to examine the

212 behavior of the Golgi during later stages of pollen tube reception, we used the synergid-
213 expressed Golgi marker line (*LRE*$_{pro}$*::Man49-mCherry*) and pollen that was expressing GFP
214 (*Lat52*$_{pro}$*::GFP*). In all cases, the Golgi marker remained randomly distributed throughout the
215 synergid cells, even after pollen tube rupture (Figures 2C-D, Movies S3 and S4, n=106). These
216 results indicate that the accumulation of NTA-GFP at the filiform apparatus during pollen tube
217 reception is not linked to mass redistribution of Golgi.
218
219 **Endosomes accumulate at the filiform apparatus during pollen tube reception**
220 A signal from the arriving pollen tube seems to trigger the movement of NTA-GFP out of the
221 Golgi-associated compartments. It is possible that pollen tube arrival triggers other changes to
222 synergid subcellular organization. We previously reported the localization of synergid-expressed
223 markers for the ER, peroxisome, endosome and the trans-Golgi Network (TGN) in unfertilized
224 ovules *in vivo* using confocal laser scanning microscopy (Jones et al., 2018). Before pollen tube
225 arrival, SP-mCherry-HDEL (an ER-associated marker), mCherry-SKL (a peroxisome-associated
226 marker), and mCherry-RabA1g (a recycling endosome-associated marker) were all distributed
227 evenly throughout synergid cells (Figures S2-S4 and 3A; (Jones et al., 2018). The TGN-
228 associated marker SYP61 exhibited two types of distribution patterns before pollen tube arrival:
229 in type 1 synergids, the marker accumulated near the filiform apparatus, whereas type 2
230 synergids displayed a punctate distribution pattern throughout the cells (Figure S3; (Jones et al.,
231 2018). During pollen tube reception, no change was seen in the TGN marker distribution in
232 either type of synergids (Figure S3, C-D, Movies S5 and S6). Likewise, the ER and peroxisome
233 markers maintained a diffuse distribution throughout the synergids and did not accumulate at
234 the filiform apparatus (Figures S2 and S4, Movies S7-10). In contrast, we detected a more
235 dynamic behavior of the endosome marker during pollen tube reception. Endosomes are
236 membrane-bound compartments that are involved in the endocytic membrane transport
237 pathway from the plasma membrane to the vacuole. Endosomes also transport molecules from

238 the Golgi and either continue to the vacuole or recycle back to the Golgi (Stoorvogel et al.,
239 1991). We previously reported that mCherry-RabA1g is distributed throughout synergid cells
240 and had some overlap with NTA-GFP in synergids of unpollinated ovules (Jones et al., 2018).
241 Using the semi-*in vivo* system, we confirmed that before pollen tube arrival, mCherry-RabA1g
242 distributed throughout synergid cells (Figure 3A). Interestingly, as pollen tubes approached, the
243 endosome marker started to accumulate in the filiform apparatus region of the synergid cells
244 (Figures 3A and B). By the time pollen tube reception was completed, most of the endosome
245 signal was concentrated at or near the filiform apparatus (Figures 3B-F and S5, Movies S11 and
246 S12). These results indicate that the RabA1g endosome compartments have a distinct response
247 to pollen tube arrival and may play a role in facilitating the intercellular signaling pathway that
248 occurs between the synergids and the pollen tube.
249
250
251 **Pollen tube-independent targeting of NTA to the filiform apparatus is not toxic to the**
252 **synergids**
253 The selective targeting of NTA-GFP from the Golgi to the filiform apparatus during pollen tube
254 arrival (Figures 1 and 2) suggests that NTA trafficking to the pollen tube/synergid interface is
255 important for the intercellular communication process that occurs between the pollen tube and
256 synergids. In *nta-1* mutants, around 30% of ovules display pollen tube overgrowth and fail to
257 complete double fertilization, but the other 70% are fertilized normally (Kessler et al., 2010).
258 This indicates that NTA is not absolutely required for pollen tube reception, but may function as
259 a modifier of the signaling pathway. Since FER signaling in the synergids leads to cell death as
260 pollen tube reception is completed (Huck et al., 2003; Rotman et al., 2003; Escobar-Restrepo et
261 al., 2007), NTA trafficking to the filiform apparatus could be a mechanism to regulate this death
262 and would thus require sequestration of “toxic” NTA in the Golgi before pollen tube arrival. To
263 test this hypothesis, we took advantage of sequence variation leading to differential subcellular

264 localization of MLO proteins to manipulate the subcellular localization of NTA. When expressed
265 in synergids, other proteins from the Arabidopsis MLO family have different subcellular
266 localization patterns, indicating that specific sequences within the MLOs direct them to different
267 parts of the secretory system (Jones and Kessler, 2017). MLO1-GFP localizes in the filiform
268 apparatus when it is ectopically expressed under control of the synergid-specific *MYB98*
269 promoter and cannot complement the *nta-1* pollen tube reception phenotype (Jones et al., 2017,
270 and Figure 4B). Domain swaps between different regions of NTA and MLO1 revealed that the
271 C-terminal cytoplasmic tail including the CaMBD of MLO1 (NTA-MLO1^{CTerm}, see diagram in
272 Figure 4C) was sufficient to direct the fusion protein to the filiform apparatus region of the
273 synergids, in a pattern very similar to MLO1-GFP (Figure 4B). Quantification of the GFP signal
274 along the length of the synergids from the chalazal end to the filiform apparatus in the NTA-
275 GFP, NTA-MLO1^{Cterm}-GFP, and MLO1-GFP confirmed that the MLO1 tail was sufficient to
276 cause NTA protein to accumulate at the filiform apparatus (Figure 4D). In all MLO1-GFP and
277 NTA-MLO1^{Cterm}-GFP ovules, the majority of GFP signal was detected in the lower 20-40% of the
278 synergids and most of the signal overlapped with the diffuse FM4-64 staining in the filiform
279 apparatus (Figure 4E). In contrast, wild-type NTA-GFP is excluded from the filiform apparatus
280 (Figure 4A and (Jones et al., 2017).
281
282 The successful manipulation of NTA subcellular localization provided a tool for determining the
283 functional relevance of NTA redistribution. We transformed the NTA-MLO1^{CTerm}-GFP construct
284 into *nta-1* plants and used the percentage of unfertilized ovules as a measurement for the ability
285 of the fusion construct to complement the *nta-1* phenotype of unfertilized ovules caused by
286 pollen tube overgrowth (Kessler et al., 2010). Synergid-expression of NTA-MLO1^{CTerm}-GFP
287 rescued the *nta-1* pollen tube reception phenotype (Figure 4F), indicating that 1) the MLO1^{CTerm}
288 domain is functionally equivalent to the NTA^{CTerm} domain when the protein is localized in the

289 filiform apparatus and 2) premature targeting of NTA to the filiform apparatus is not toxic to
290 synergid cells.
291
292 **Disrupting the NTA CaMBD compromises NTA's ability to accumulate at the filiform**
293 **apparatus during pollen tube reception**
294 The dramatic differences in protein localization between NTA-GFP and NTA-MLO1^{CTerm}-GFP
295 revealed that the C-terminal cytoplasmic domain of NTA contains sequences that cause NTA to
296 be sequestered in the Golgi before pollen tube arrival and possibly also to allow for directed
297 transport to the filiform apparatus in response to signals from the arriving pollen tube. The C-
298 terminal cytoplasmic domains of MLO proteins contain a predicted CaMBD followed by an
299 unconserved tail of variable length (Devoto et al., 1999; Kim et al., 2002b; Kim et al., 2002a). A
300 comparison of C-terminal domains (Figure 5A) revealed that NTA and MLO1 share the
301 conserved 20 amino acid 1-8-14 CaM binding motif of hydrophobic residues interspersed with
302 basic residues that define the MLO CaMBD (Kim et al., 2002b), but have different residues
303 surrounding the conserved tryptophan that has been shown to necessary for CaM binding in
304 MLO proteins (Kim et al., 2002b; Kim et al., 2002a). In addition, NTA and MLO1 have different
305 length C-terminal tails after the CaMBD (Figure 5A). In order to determine if the C-terminal tail
306 after the CaMBD is necessary for NTA sequestration in the Golgi before pollen tube arrival, we
307 made a GFP fusion with NTA truncated just after the predicted CaMBD (NTA$^{\Delta 481}$, Figure 5A)
308 expressed under control of the synergid-specific MYB98 promoter. This construct
309 complemented the *nta-1* pollen tube reception phenotype and localized in the Golgi before
310 pollen tube arrival (Figure 5C and 5E), revealing that the C-terminal tail after the CaMBD is not
311 necessary for NTA sequestration or function. We next tested whether disruption of the CaMBD
312 would affect NTA localization and/or function. A point mutation in the conserved tryptophan
313 necessary for CaM-binding in other CaMBDs (Arazi et al., 1995; Yamada et al., 1995; Kim et al.,
314 2002b) was introduced into our NTA-GFP expression construct (NTA^{W458A}, Figure 5A) and

315 transformed into the *nta-1* background. In contrast to wild-type NTA and $NTA^{\Delta 481}$, which result
316 in an even higher fertility in *nta-1* mutants than in the Ws controls, NTA^{W458A} only partially
317 complemented the *nta-1* fertility phenotype (Figure 5E). Before pollen tube arrival, NTA^{W458A} co-
318 localizes with a Golgi marker in synergids similar to wild-type NTA (Figure 5D and Figure S6).
319 However, during pollen tube reception, NTA^{W458A} displays different accumulation patterns that
320 correlate with the ability of the pollen tube to rupture. In our semi-*in vivo* system, ovules with
321 normal pollen tube rupture had at least partial NTA^{W458A} accumulation at the filiform apparatus,
322 while ovules with pollen tube overgrowth did not accumulate NTA^{W458A} at the filiform apparatus
323 (Figure 6). These data reveal that an intact CaMBD enhances NTA's redistribution to the filiform
324 apparatus during pollen tube reception and that NTA accumulation at the filiform apparatus
325 promotes pollen tube rupture, while the C-terminal tail after the CaMBD is dispensable for NTA
326 function.
327
328 The influence of the CaMBD on NTA accumulation at the filiform apparatus could indicate a
329 connection with the calcium oscillations that occur in synergids during signaling with the arriving
330 pollen tube. The receptor-like kinase FER and the GPI-anchored protein LRE are filiform-
331 localized proteins that interact with each other and form a co-receptor for signals from the
332 arriving pollen tube (Escobar-Restrepo et al., 2007; Li et al., 2015; Liu et al., 2016). *fer* and *lre*
333 mutant ovules fail to initiate synergid calcium oscillations at pollen tube arrival and have highly
334 penetrant pollen tube overgrowth phenotypes (Ngo et al., 2014). In *nta-1* mutant ovules,
335 synergids have dampened calcium oscillations and around 30% of ovules carrying the mutation
336 display pollen tube overgrowth (Kessler et al., 2010; Ngo et al., 2014). In both *fer-1* and *lre-7*
337 backgrounds, NTA-GFP does not accumulate at the filiform apparatus in response to signals
338 from the pollen tube (Figure S7 and Kessler, 2010), placing NTA accumulation at the filiform
339 apparatus downstream of both FER and LRE and the calcium oscillations conditioned by these
340 proteins.

341

342 **Discussion**

343 **Synergids respond to a signal from the approaching pollen tube**

344 Successful pollination and production of seeds requires a series of signaling events between the
345 male gametophyte (pollen tube) and both sporophytic and gametophytic cells of the female. In
346 this study, we used live imaging to characterize dynamic subcellular changes that occur in the
347 synergid cells of the female gametophyte in response to the arrival of the pollen tube. We
348 showed that both the NTA protein and endosomes are actively mobilized to the filiform
349 apparatus region where male-female communication occurs during pollen tube reception
350 (Figure 7). Disruption of NTA's CaMBD partially compromised NTA redistribution and function in
351 pollen tube reception, revealing that Ca^{2+} may play a role in the synergid response to the signal
352 from the pollen tube.

353

354 The polar accumulation of the RabA1g endosome marker, but not a Golgi marker (Man49-GFP),
355 near the filiform apparatus during pollen tube reception suggests a change in synergid secretory
356 system behavior that is triggered by the approaching pollen tube. Our results with the ER, Golgi,
357 TGN, and peroxisome markers indicate that the mobilization of the RabA1g endosomes toward
358 the approaching pollen tube is not just a symptom of FER signaling triggering synergid cell
359 death that leads to mass disruption of subcellular compartments. Trans-Golgi Network/Early
360 endosomes (TGN/EEs) have been shown to be involved in the trafficking of both secretory and
361 endocytic cargo (Viotti et al., 2010). RabA1g is present in endosomes that are highly sensitive to
362 Brefeldin A in roots, suggesting that they could function as recycling endosomes (Geldner et al.,
363 2009). While the resolution of our live imaging system did not allow us to determine whether
364 NTA completely co-localizes with this compartment, it is tempting to speculate that the RabA1g
365 endosomes are mediating the polar movement of NTA to the filiform apparatus region.

366 Alternatively, these endosomes could be transporting other signaling molecules either to or from
367 the filiform apparatus.
368
369 **Signal-mediated protein trafficking**
370 Signal-mediated regulation of protein trafficking is an elegant mechanism to control the delivery
371 of molecules to the precise location where they are needed for critical signaling events that
372 occur over relatively short time frames. Selective protein targeting similar to NTA movement in
373 response to pollen tube arrival has also been observed during cell-to-cell communication
374 between the egg and sperm cells in Arabidopsis. After pollen tube reception and release of the
375 sperm cells, a signal from the sperm and/or the degenerated synergid cell causes the egg cell to
376 secrete EGG CELL 1 (EC1) peptides that have been stored in punctate compartments in the
377 egg cytoplasm toward the sperm cells. The sperm cells perceive the EC1 signal and, in turn,
378 mobilize the gamete fusogen HAPLESS2/GENERATIVE CELL SPECIFIC1 (HAP2/GCS1) from
379 a cytoplasmic compartment to the cell surface (Sprunck et al., 2012). This controlled movement
380 of proteins that have already been translated and stored facilitates a quick response to activate
381 the egg and sperm for fertilization. Likewise, NTA mobilization to the filiform apparatus region of
382 the synergids as the pollen tube arrives could play a role in sending a signal to the pollen tube
383 that leads to the mobilization of pollen tube proteins that allow the pollen tube to rupture and
384 release the sperm cells. For example, proteins that regulate the integrity of the tip of the pollen
385 tube could be quickly delivered after the “arrival” signal from the synergid is perceived. Recent
386 work on the role of the pollen-expressed ANXUR1 and 2 and BUDDHA PAPER SEAL1 and 2
387 receptor-like kinases in pollen tube tip integrity support this hypothesis. During pollen tube
388 growth through the female tissues, RALF4 and RALF19 peptides that are secreted from pollen
389 tubes act as ligands for ANX1/2 and BPS1/2 to promote tip growth, while RALF34 secreted from
390 the synergids displaces RALF4 and 19 from the receptors leading to subcellular changes that
391 result in pollen tube rupture (Ge et al., 2017).

392

393 **Calcium and NTA movement**

394 Our study revealed that an intact CaMBD facilitates the trafficking of NTA from the Golgi to the
395 filiform apparatus in response to a stimulus from the approaching pollen tube and that the
396 FER/LRE co-receptor is necessary for perceiving this stimulus. This result provides an intriguing
397 link to Ca^{2+} since the polar accumulation of NTA-GFP at the filiform apparatus region occurs in a
398 similar time frame to the FER/LRE-dependent $[Ca^{2+}]_{cyto}$ spiking in the synergids during pollen
399 tube reception (Denninger et al., 2014; Ngo et al., 2014). Subcellular Ca^{2+} spiking occurs in
400 plant responses to both biotic and abiotic external stimuli. Notably, $[Ca^{2+}]_{cyto}$ oscillations occur
401 during pollen tube-synergid interactions, egg-sperm interactions, and in biotrophic interactions
402 between plant cells and both beneficial and harmful microbes (reviewed in Chen et al., 2015). In
403 most cases, the mechanism for decoding $[Ca^{2+}]_{cyto}$ spikes into a cellular response is not known,
404 but Ca^{2+}-binding proteins such as calmodulin (CaM) and CaM-like proteins could play a role in
405 relaying Ca^{2+} signals (Chin and Means, 2000). In *nta-1* mutants, the $[Ca^{2+}]_{cyto}$ oscillations still
406 occur, but at a lower magnitude than in wild-type synergids, suggesting that NTA could be
407 involved in modulating Ca^{2+} flux (Ngo et al., 2014). The source of Ca^{2+} during these oscillations
408 is not known, but it is possible that NTA regulates Ca^{2+} channels to regulate the flow of Ca^{2+}ions
409 into or out of the apoplast near the filiform apparatus.

410

411 Ca^{2+} has also been linked to regulation of endomembrane trafficking (reviewed in Himschoot et
412 al., 2017). In animals, CaM plays a role in regulating vesicle tethering and fusion (Burgoyne and
413 Clague, 2003), and in plants CaM-like proteins are associated with endosomal populations
414 (Ruge et al., 2016). Thus, it is possible that the CaMBD in NTA is critical for the precise
415 targeting of NTA in response to pollen tube arrival. Another mechanism that has been proposed
416 for Ca^{2+} regulation of protein targeting is that electrostatic interactions between Ca^{2+} and anionic
417 phospholipids in specific domains of the plasma membrane regulate vesicle fusion and

418 differential recruitment of proteins to these domains (Simon et al., 2016; Platre et al., 2018). The
419 filiform apparatus of the synergids is distinctive from the plasma membrane in other parts of the
420 synergid and likely has a unique phospholipid composition that could play a role in recruiting
421 NTA to this domain. Whether NTA movement is a cause or consequence of $[Ca^{2+}]_{cyto}$ spiking
422 requires more live imaging experiments at a higher time resolution to determine if NTA
423 redistribution happens before or after the initiation of $[Ca^{2+}]_{cyto}$ spiking.
424
425 **Cell death and pollen tube reception**
426 MLOs were first discovered in barley as powdery mildew resistance genes (Buschges et al.,
427 1997). *mlo* mutants in both monocots and dicots are resistant to powdery mildew infection,
428 indicating that the MLO proteins are required for infection. These mutants also have ectopic cell
429 death, indicating that one function of MLO proteins is to negatively regulate cell death
430 (Panstruga, 2005). Pollen tube reception is catastrophic for both the pollen tube and the
431 receptive synergid cell: both cells die as a result of successful male-female signaling and
432 delivery of the male gametes. The timing of synergid degeneration remains under debate, with
433 some studies suggesting that it occurs upon pollen tube arrival at the synergid and others
434 concluding that it occurs concurrently with pollen tube rupture (Sandaklie-Nikolova et al., 2007;
435 Hamamura et al., 2011; Leydon et al., 2015). Our live imaging experiments with both NTA-GFP
436 and the subcellular compartment reporters suggest that the synergid cells are still alive and
437 regulating their secretory systems up to the point of pollen tube rupture. Given the function of
438 the “powdery mildew” members of the MLO gene family in preventing cell death, it is possible
439 that one role of NTA is to prevent early degeneration of the synergids. An interesting parallel
440 between powdery mildew infection and pollen tube reception is that, in both cases, an MLO
441 protein accumulates at the site of interaction with a tip-growing cell. In the powdery mildew
442 system, active transport of proteins and lipids to penetration site leads to membrane remodeling
443 and establishment of the extrahaustorial membrane which separates the plant cytoplasm from

444 the invading fungal hyphae (Huckelhoven and Panstruga, 2011). Although the relationship
445 between the arriving pollen tube and the filiform apparatus has not been established, it is
446 possible that similar reorganization occurs in the filiform apparatus during signaling with the
447 pollen tube. In both cases, perhaps an MLO protein is needed in these special membrane
448 regions to stabilize the cell and prevent precocious cell death. Our result that premature delivery
449 of NTA (in the NTA-MLO1^{CTerm} domain swap construct) to the filiform apparatus region of the
450 cell does not disrupt pollen tube reception is consistent with this hypothesis, since other
451 signaling processes occurring in the synergids during communication with the arriving pollen
452 tube would likely not be triggered by simply moving NTA to the filiform apparatus in the absence
453 of a pollen tube.
454
455 In this study, we showed that signals from an approaching pollen tube trigger the movement of
456 NTA out of the Golgi and to the filiform apparatus and that this redistribution is correlated with
457 pollen tube reception. However, filiform apparatus-localization of the NTA-MLO1^{CTerm} fusion
458 protein was able to complement the *nta-1* mutant phenotype, indicating that the final localization
459 of the NTA protein may be more important than the active trafficking from the Golgi. Future work
460 will focus on determining the mechanism through which NTA polarly accumulates at the filiform
461 apparatus and on identifying the signals from the pollen tube that lead to important subcellular
462 changes in the synergids during pollen tube reception.
463

464 **Materials and methods**

465 **Plant materials and growth conditions**

466 *Arabidopsis thaliana* lines expressing *NTA$_{pro}$::NTA-GFP*, *MYB98$_{pro}$::NTA-GFP*,
467 *MYB98$_{pro}$::MLO1-GFP*,Golgi-associated marker (Man49-mCherry), ER-associated marker (SP-
468 mCherry-HDEL), TGN-associated marker (SYP61-mCherry), peroxisome-associated marker
469 (Peroxisome-mCherry) and recycling endosome-associated marker (mCherry-RabA1g), were
470 generated and described in previous publications (Kessler et al., 2010; Liu et al., 2016; Jones et
471 al., 2017; Jones et al., 2018). Pollen tube marker lines, *ACA9::DsRed* (Boisson-Dernier et al.,
472 2008) and *Lat52::GFP* (Palanivelu and Preuss, 2006) were generously provided by Dr. Aurelien
473 Boisson-Dernier and Dr. Ravi Palanivelu. *fer-1* seeds were provided by Dr. Ueli Grossniklaus
474 and *lre-7* seeds were provided by Dr. Ravi Palanivelu. Seeds were sterilized and plated on ½-
475 strength Murashige and Skoog (MS) plates. All plates were sealed and stratified at 4˚C for two
476 days, and then transferred to the growth chamber (long day conditions, 16 h of light and 8 h of
477 dark at 22˚C) for germination and growth. After 5-7 days, seedlings were transplanted to soil.
478 Seeds from transformed lines were sterilized and plated on ½ MS plate with 20 mg/L
479 hygromycin for selection of transgenic seedlings, which were then transplanted to soil and
480 grown in long days.

481

482 **Live Imaging of Pollination Using a Semi-*in vivo* Pollen Tube Guidance Assay**

483 The semi-*in vivo* system of pollen tube reception was modified from (Palanivelu and Preuss,
484 2006). Approximately 150 µL of pollen germination media (5 mM KCl, 1 mM $MgSO_4$, 0.01%
485 (w/v) H_3BO_3, 5 mM $CaCl_2$, 20% sucrose, 1.5% agarose, and adjusted pH to 7.5 with KOH) was
486 poured into a Glass Bottom Culture Petri Dish (MatTek Corporation, P35G-1.0-20-C) and
487 spread out using a pipette. Pistils were emasculated and 2 d later were hand pollinated with
488 *ACA9::DsRed* or *Lat52::GFP* pollen and returned to the growth chamber. Approximately 1 h
489 after pollination, pistils were removed from plants and placed on double sided tape on a glass

490 slide. Stigmas were cut using single-sided razor blade and placed on pollen germination media
491 using forceps. 8-10 ovules were arranged around the cut style and the petri dish was returned to
492 the growth chamber. After 4-6 h, pollen tubes grew through the stigma and style and emerged
493 near the ovules. Imaging commenced when the pollen tubes approached ovules. Time-lapse
494 images were acquired at 5 min intervals by spinning disk confocal microscopy using an Andor
495 Revolution XD platform with a Yokogawa CSU-X1-A1 scanner unit mounted on an Olympus IX-
496 83 microscope and a 20X/0.5 NA objective (Olympus). An Andor iXon Ultra 897BV EMCCD
497 camera was used to capture GFP fluorescence (488-nm excitation) and red fluorescent protein
498 (dsRed or mCherry) fluorescence (561-nm excitation).
499
500 For each experimental condition, at least 60 ovules were imaged over the time course from
501 pollen tube approaching the ovule to completion of pollen tube reception (pollen tube rupture to
502 release the sperm cells). Neighboring ovules that did not attract pollen tubes were imaged at the
503 same time and served as controls for photoxicity.
504
505 **Confocal laser scanning microscopy (CLSM)**
506 CLSM to examine MLO variant subcellular localization was performed on ovules dissected 2 d
507 after emasculation. FM4-64 staining was performed according to the protocol described in
508 (Jones et al., 2017). CLSM was done using either a Nikon A1Rsi inverted confocal microscope
509 according to (Yuan and Kessler, 2019) or a Leica SP8 upright confocal microscope according to
510 (Jones et al., 2017).
511
512 **Quantification of fluorescence signal intensity**
513 Two-channel images were adjusted for brightness and contrast using Fiji (Schindelin et al.,
514 2012). Then, they were input to NIS-Elements software (Ver. 5.02) to measure the fluorescence
515 signal intensity. A line that spanned from the chalazal end to the filiform apparatus end of the

516 synergid was used for the signal intensity measurements. For a more accurate representation of
517 the total area of the synergid, signal intensities were recorded along the same length line at five
518 parallel position within the synergid cell. Finally, all the measurement data were output as Excel
519 files. Graphs and statistical analysis were performed with Prism software (www.graphpad.com).
520

521 **Video processing**

522 Images were filtered to remove the noise and cropped using Fiji (Version 2.0.0). QuickTime
523 Player (Version 10.5) was used for movie editing and time-lapse analyses.
524

525 **Cloning and Generation of Transgenic Lines**

526 PCR amplification with PHUSION High-Fidelity Polymerase (NEB, M0535S) or Q5 High-Fidelity
527 DNA Polymerase (NEB, M0419S) were used to generate the following constructs in this study.
528 Genes were amplified with primers that had attB1 and attB2 sites for recombination via BP
529 reaction into the Gateway-compatible entry vector pDONR207. Full-length NTA entry vectors
530 used in this study was generated as described previously (Jones et al., 2017) . NTA truncations
531 were amplified using NTA full-length entry vector as a template with forward primer NTA-FattB1
532 and the following reverse primers: NTA450-RattB2 and NTA481-RattB2 (See all primer
533 sequences in Table S1). The NTA^{W458A} point mutation was generated using the same *NTA*
534 template and amplifying two fragments of *NTA* with desired point mutations introduced into the
535 primers: NTA-FattB1 + NTAW458A-R and NTAW458A-F + NTA-RattB2. The two fragments
536 were purified and pasted together with overlaps using a PCR-pasting protocol. The NTA-
537 $MLO1^{CTerm}$ construct was generated using the full-length entry vectors of NTA and MLO1 used
538 in previous study (Jones et al., 2017) as templates and amplifying two fragments of *NTA* and
539 *MLO1* using the two pairs of primers: NTA-FattB1 +NTA-R19 and MLO1-F + MLO1-RattB2. The
540 two fragments were purified and pasted together with overlaps using a PCR-pasting protocol.
541 The NTA-$MLO1^{CTerm}$-RNIKCD construct was generated using the full-length expression vector of

542 MYB98$_{pro}$-NTA-MLO1^{CTerm}-GFP as template and amplifying two fragments with NTA-MLO1^{CTerm}
543 and GFP-RNIKCD with five glycines as linker using the two pairs of primers: NTA-FattB1 +
544 MLO1-Gly5-GFP-R and MLO1-Gly5-GFP-F + GFP-RNIKCD-RattB2. The two fragments were
545 purified and pasted together with overlaps using a PCR-pasting protocol. The coding sequence
546 from both truncations and the point mutation and the fusion sequences were fully sequenced in
547 entry vectors. All entries were then recombined via LR reactions into the pMDC83 backbone
548 with the MYB98$_{pro}$ (Muller et al., 2016) to drive expression of each NTA variant in synergid cells
549 with a C-terminal GFP fusion.
550
551 For *nta-1* complementation assay and co-localization analyses, expression vectors were
552 transformed into the *Agrobacterium tumefaciens* strain GV3101 and transformed into the *nta-1*
553 mutant background or the Col-0 background (for co-localization combinations, Col-0 stably
554 expressing the Golgi or TGN synergid secretory markers was used for transformation) via the
555 floral-dip method (Bent, 2006). Stable transgenic lines were selected using their respective
556 selections described above. Homozygous T2 lines were used in *nta-1* complementation assay
557 and co-localization imaging in the synergid was done in a T1 analysis. The NTApro::NTA-GFP
558 construct described in (Kessler et al., 2010) was introduced into the *lre-7* background by floral
559 dip as described above.
560
561 ***nta-1* Complementation Assays**
562 3-4 independent insertion lines for each construct were taken to the T2 generation and
563 screened for homozygosity using fluorescence microscopy to ensure transgene expression in
564 synergids of every ovule. Unfertilized vs. fertilized ovule counts from self-pollinated flowers were
565 assessed in at least five plants of each insertion line and compared to *nta-1*, Wassilewskija (Ws-
566 2; wildtype), and the previously published full-length NTA (MYB98$_{pro}$::NTA-GFP in *nta-1*
567 background, (Jones et al., 2017). Ovule counts were statistically analyzed using Prism with

568 significance determined using a Student's *t*-test. Comparisons of the NTA variants were made
569 to full-length NTA and the *nta-1* mutant.
570
571 **Acknowledgements**
572 We thank Patrick Day for technical assistance and Rachel Flynn and Thomas Davis for helpful
573 discussions and comments on the manuscript. This work was supported by funds from NSF
574 IOS-1733865 to SAK, Purdue University Start-up funds to SAK, and a grant from the Oklahoma
575 Center for the Advancement of Science and Technology #PS14-008 to SAK. Spinning disk
576 confocal microscopy in the Staiger laboratory was supported, in part, by an award from the
577 Office of Science at the US Department of Energy, Physical Biosciences Program, under
578 contract number DE-FG02-09ER15526 to CJS.
579
580 **Author Contributions**
581 JY, YJ, DSJ, and SAK conceived and designed the experiments. JY, YJ, DSJ, NL, and WZ
582 performed the experiments. JY, YJ, DSJ, and SAK analyzed the data. JY, YJ, DSJ, and SAK
583 wrote the manuscript, and all authors revised and approved the final manuscript.
584
585 **Competing Interests**
586 The authors declare no competing interests.
587
588
589
590
591 **Figure Legends**
592 **Figure 1. NTA-GFP accumulates at the filiform apparatus as the pollen tube approaches.**
593 (A) Diagram of a mature *Arabidopsis thaliana* ovule and embryo sac, modified from Jones et al,

594 2018. CC, Central Cell; Syn, Synergid Cells; EC, Egg Cell; An, Antipodal cells; FA, Filiform
595 Apparatus (B, C) Live imaging of pollen tube (PT) reception using NTA-GFP labeled synergids
596 (green signal) and *ACA9::DsRed* pollen tubes (magenta signal). (B) Polar NTA-GFP
597 accumulation at the filiform apparatus (FA) occurred in ovules that attracted a pollen tube
598 (ovules with yellow stars), while polar NTA-GFP accumulation did not occur in ovules without
599 pollen tube attraction (ovules with white stars). (C) Time-lapse imaging of NTA-GFP
600 accumulation during pollen tube reception. (D) Quantification of NTA-GFP signal along the
601 length of the synergid from chalazal end (0μm) to FA end (33μm) at 0min, 25min, 50min, 75min,
602 and 100min timepoints, respectively. (E) 6 more examples of the quantification of NTA-GFP
603 signal along the length of synergids after pollen tube arrival. (F) Quantification of the percentage
604 of ovules with different NTA accumulation patterns under the same imaging conditions. Bars=50
605 μm (B and C).
606
607 **Figure 2. The Golgi marker is randomly distributed throughout synergids during pollen**
608 **tube reception.** (A) NTA-GFP (green signal) and Golgi-mCherry signals (magenta signal) are
609 evenly distributed along the length of the synergid and co-localized within synergid cells before
610 pollen tube arrival. (B) After pollen tube arrival, NTA-GFP accumulated at the FA, but Golgi-
611 mCherry did not accumulate at the FA. (C) Live imaging of Golgi-mCherry during reception of
612 *Lat52::GFP* labeled pollen tubes. (D) Quantification of Golgi-mCherry signal along the length of
613 synergids shown in (C) before and after pollen tube arrival. Bars=30μm (A-B), 50μm (C).
614
615 **Figure 3. RabA1g endosomes polarly accumulate toward the filiform apparatus during**
616 **pollen tube reception.** (A) RabA1g-mCherry endosome marker (magenta signal) accumulates
617 at the FA region in response to pollen tube arrival (ovule with yellow star). The ovule with no
618 pollen tube attraction (white star) serves as a negative control imaged under the same
619 conditions. (B) Higher magnification of the micropylar region of starred ovule in (red box in panel

620 A). (C) Timing of RabA1g-mCherry polar accumulation during pollen tube arrival. Bars=50μm.
621 (D) Quantification of RabA1g-mCherry signal along the length of synergids during pollen tube
622 reception. Synergid cell from chalazal end to filiform apparatus (FA) end was defined from 0 to
623 33 μm in length. (E) 6 more examples of the quantification of RabA1g-mCherry signal after
624 pollen tube arrival. (F) Quantification of ovule percentage with RabA1g endosome marker
625 throughout the synergids (gray bars) or with polar accumulation at or near the filiform apparatus
626 (black bars).
627
628 **Figure 4. Targeting of NTA to the filiform apparatus before pollen tube arrival is not toxic**
629 **to synergid cells.** (A-C) Localization patterns of MYB98 promoter driven MLO-GFP variants
630 (green signal) in synergids of mature virgin ovules stained with FM4-64 (magenta signal) to reveal
631 the outline of the synergid and the filiform apparatus (FA, diffuse magenta signal). Bars = 10 μm.
632 (D) Quantification of the GFP intensity of the MLO variants in A-C along the length of the synergids.
633 (E) Percentage of ovules showing MLO-GFP signal throughout the synergids (100% of length), in
634 the FA only (20% of length) and the region surrounding and including the FA (40% of length). (F)
635 Scatter plot of unfertilized ovule percentages in homozygous plants of pMYB98::MLO-GFP in *nta-*
636 *1* mutants to assess the ability of the MLO-GFP constructs to complement *nta-1*. WS,
637 Wassilewskija. Significance was determined by a Student's *t*-test (****, $P < 0.0001$; *, $P = 0.0281$;
638 and ns, $P = 0.2020$).
639
640 **Figure 5. Analysis of NTA variants expressed in synergids of *nta-1*.** (A) Alignment of MLO1
641 and NTA C-terminal domains after the seventh membrane span. Red bars highlight the CaMBD;
642 W458A and Δ481 indicate the point mutation in NTA and the deletion point, respectively ; a.a.,
643 amino acid. (B-D) NTA (variant)-GFP (green) distribution in synergid cells of unfertilized ovules
644 stained with FM4-64 (magenta signal). Bar = 10 μm. (E) Complementation analysis of NTA
645 variants in T2 plants homozygous for $MYB98_{pro}$::NTA(variant)-GFP constructs in *nta-1* mutants.

646 Adjusted P values from a Student's *t*-test are as follows: **** indicates $P < 0.0001$; *** indicates
647 $P = 0.001$ to 0.0001; and ns indicates $P > 0.05$.
648
649 **Figure 6. A point mutation in the CaMBD (NTA^{W458A}) affects filiform apparatus**
650 **accumulation of NTA and pollen tube reception.** (A) NTA^{W458A}-GFP has 3 different
651 localization patterns in response to PT arrival under semi *in-vivo* conditions. Bar=50 µm (B)
652 Quantification of GFP signal intensity in NTA^{W458A} synergids during pollen tube reception. (C)
653 Analysis of NTA^{W458A}-GFP distribution patterns in ovules with successful (PT bursting) and
654 unsuccessful (no PT or PT overgrowth (PT OG)) pollen tube reception.
655
656 **Figure 7. Subcellular dynamics in synergids during pollen tube reception.** (A) Pollination
657 using a semi-*in vivo* pollen tube guidance assay. (B) Before pollen tube arrival, NTA is in a
658 Golgi-associated compartment and RabA1g endosomes are distributed throughout the
659 synergids. (C) As a pollen tube arrives, NTA and RabA1g endosomes move toward the filiform
660 apparatus (FA). NTA accumulation is dependent on signaling from the FER receptor like
661 kinase, which acts in a complex with LRE. Abbreviations: CC, Central Cell; Syn, Synergid cells;
662 EC, Egg Cell; An, Antipodal cells; nuc, Nucleus; FA, Filiform Apparatus.
663
664
665 **Supplemental Materials**
666 **Supplementary figure 1.** NTA-GFP does not polarly accumulate at the filiform apparatus in
667 synergids without pollen tube attraction.
668 **Supplementary figure 2.** Peroxisomes do not exhibit polar accumulation at the FA during
669 pollen tube reception.
670 **Supplementary figure 3.** Trans-Golgi marker distribution in synergids does not change in
671 response to pollen tube reception.

672 **Supplementary figure 4.** ER marker distribution in synergids does not change in response to
673 pollen tube reception.
674 **Supplementary figure 5**. Additional examples of the polar accumulation of RabA1g endosomes
675 during pollen tube reception.
676 **Supplementary figure 6.** NTA^{W458A} co-localizes with Golgi marker in synergid cells before pollen
677 tube arrival.
678 **Supplementary figure 7**. NTA-GFP polar accumulation requires FER and LRE.
679
680 **Supplemental Movies**
681 **Supplementary movie 1.** NTA-GFP (green signal) redistributes to filiform apparatus region as
682 ACA9::DsRed labeled pollen tube (magenta signal) approaches.
683 **Supplementary movie 2.** NTA-GFP (green signal) redistributes to filiform apparatus region
684 during pollen tube reception (GFP channel only, same movie as S1).
685 **Supplementary movie 3.** Golgi-mCherry signals (magenta signal) are evenly distributed along
686 the length of the synergid as Lat52::GFP labeled pollen tube (green signal) approaches.
687 **Supplementary movie 4.** Golgi-mCherry signals (magenta signal) are evenly distributed along
688 the length of the synergid during pollen tube reception (mCherry channel only, same movie as
689 S3).
690 **Supplementary movie 5.** The trans-Golgi marker SYP61-mCherry (magenta signal) is localized
691 toward the micropyle region of synergid cells both before and after pollen tube (green signal)
692 arrival.
693 **Supplementary movie 6.** The trans-Golgi marker SYP61-mCherry (magenta signal) is localized
694 toward the micropyle region of synergid cells during pollen tube reception (mCherry channel
695 only, same movie as S5).
696 **Supplementary movie 7.** Before and after pollen tube (green signal) arrival, the ER marker SP-
697 mCherry-HDEL (magenta signal) is distributed throughout synergid cells.

698 **Supplementary movie 8.** The ER marker SP-mCherry-HDEL (magenta signal) is distributed
699 throughout synergid cells (mCherry channel only, same movie as S7).
700 **Supplementary movie 9.** The peroxisome marker mCherry-SLK (magenta signal) does not
701 redistribute to the filiform apparatus region after pollen tube (green signal) arrival.
702 **Supplementary movie 10.** The peroxisome marker mCherry-SLK (magenta signal) does not
703 redistribute to the filiform apparatus region during pollen tube reception (mCherry channel only,
704 same movie as S9).
705 **Supplementary movie 11.** RabA1g-mCherry endosome marker (magenta signal) accumulates
706 at the filiform apparatus region in response to pollen tube (green signal) arrival.
707
708
709 **References**

710 **Arazi, T., Baum, G., Snedden, W.A., Shelp, B.J., and Fromm, H.** (1995). Molecular and
711 Biochemical-Analysis of Calmodulin Interactions with the Calmodulin-Binding Domain of
712 Plant Glutamate-Decarboxylase. Plant Physiology **108,** 551-561.
713 **Bent, A.** (2006). Arabidopsis thaliana Floral Dip Transformation Method. In Methods in
714 Molecular Biology, K. Wang, ed (Totowa, NJ: Humana Press Inc.
715 **Boisson-Dernier, A., Frietsch, S., Kim, T.H., Dizon, M.B., and Schroeder, J.I.** (2008). The
716 peroxin loss-of-function mutation abstinence by mutual consent disrupts male-female
717 gametophyte recognition. Curr Biol **18,** 63-68.
718 **Burgoyne, R.D., and Clague, M.J.** (2003). Calcium and calmodulin in membrane fusion.
719 Biochim Biophys Acta **1641,** 137-143.
720 **Buschges, R., Hollricher, K., Panstruga, R., Simons, G., Wolter, M., Frijters, A., van**
721 **Daelen, R., van der Lee, T., Diergaarde, P., Groenendijk, J., Topsch, S., Vos, P.,**
722 **Salamini, F., and Schulze-Lefert, P.** (1997). The barley Mlo gene: a novel control
723 element of plant pathogen resistance. Cell **88,** 695-705.
724 **Capron, A., Gourgues, M., Neiva, L.S., Faure, J.E., Berger, F., Pagnussat, G., Krishnan, A.,**
725 **Alvarez-Mejia, C., Vielle-Calzada, J.P., Lee, Y.R., Liu, B., and Sundaresan, V.** (2008).
726 Maternal Control of Male-Gamete Delivery in Arabidopsis Involves a Putative GPI-
727 Anchored Protein Encoded by the LORELEI Gene. Plant Cell **20,** 3038-3049.
728 **Chen, J., Gutjahr, C., Bleckmann, A., and Dresselhaus, T.** (2015). Calcium signaling during
729 reproduction and biotrophic fungal interactions in plants. Mol Plant **8,** 595-611.
730 **Chin, D., and Means, A.R.** (2000). Calmodulin: a prototypical calcium sensor. Trends Cell Biol
731 **10,** 322-328.
732 **Denninger, P., Bleckmann, A., Lausser, A., Vogler, F., Ott, T., Ehrhardt, D.W., Frommer,**
733 **W.B., Sprunck, S., Dresselhaus, T., and Grossmann, G.** (2014). Male-female
734 communication triggers calcium signatures during fertilization in Arabidopsis. Nature
735 communications **5,** 4645.

736 **Devoto, A., Piffanelli, P., Nilsson, I., Wallin, E., Panstruga, R., von Heijne, G., and Schulze-**
737 **Lefert, P.** (1999). Topology, subcellular localization, and sequence diversity of the Mlo
738 family in plants. J Biol Chem **274,** 34993-35004.
739 **Devoto, A., Hartmann, H.A., Piffanelli, P., Elliott, C., Simmons, C., Taramino, G., Goh, C.S.,**
740 **Cohen, F.E., Emerson, B.C., Schulze-Lefert, P., and Panstruga, R.** (2003). Molecular
741 phylogeny and evolution of the plant-specific seven-transmembrane MLO family. J Mol
742 Evol **56,** 77-88.
743 **Drews, G.N., and Yadegari, R.** (2002). Development and function of the angiosperm female
744 gametophyte. Annu Rev Genet **36,** 99-124.
745 **Escobar-Restrepo, J.M., Huck, N., Kessler, S., Gagliardini, V., Gheyselinck, J., Yang, W.C.,**
746 **and Grossniklaus, U.** (2007). The FERONIA receptor-like kinase mediates male-female
747 interactions during pollen tube reception. Science **317,** 656-660.
748 **Gao, C., Yu, C.K., Qu, S., San, M.W., Li, K.Y., Lo, S.W., and Jiang, L.** (2012). The Golgi-
749 localized Arabidopsis endomembrane protein12 contains both endoplasmic reticulum
750 export and Golgi retention signals at its C terminus. Plant Cell **24,** 2086-2104.
751 **Ge, Z., Bergonci, T., Zhao, Y., Zou, Y., Du, S., Liu, M.C., Luo, X., Ruan, H., Garcia-Valencia,**
752 **L.E., Zhong, S., Hou, S., Huang, Q., Lai, L., Moura, D.S., Gu, H., Dong, J., Wu, H.M.,**
753 **Dresselhaus, T., Xiao, J., Cheung, A.Y., and Qu, L.J.** (2017). Arabidopsis pollen tube
754 integrity and sperm release are regulated by RALF-mediated signaling. Science **358,**
755 1596-1600.
756 **Geldner, N., Denervaud-Tendon, V., Hyman, D.L., Mayer, U., Stierhof, Y.D., and Chory, J.**
757 (2009). Rapid, combinatorial analysis of membrane compartments in intact plants with a
758 multicolor marker set. Plant J **59,** 169-178.
759 **Hamamura, Y., Nagahara, S., and Higashiyama, T.** (2012). Double fertilization on the move.
760 Curr Opin Plant Biol **15,** 70-77.
761 **Hamamura, Y., Nishimaki, M., Takeuchi, H., Geitmann, A., Kurihara, D., and Higashiyama,**
762 **T.** (2014). Live imaging of calcium spikes during double fertilization in Arabidopsis. Nat
763 Commun **5,** 4722.
764 **Hamamura, Y., Saito, C., Awai, C., Kurihara, D., Miyawaki, A., Nakagawa, T., Kanaoka,**
765 **M.M., Sasaki, N., Nakano, A., Berger, F., and Higashiyama, T.** (2011). Live-cell
766 imaging reveals the dynamics of two sperm cells during double fertilization in
767 Arabidopsis thaliana. Curr Biol **21,** 497-502.
768 **Himschoot, E., Pleskot, R., Van Damme, D., and Vanneste, S.** (2017). The ins and outs of
769 Ca(2+) in plant endomembrane trafficking. Curr Opin Plant Biol **40,** 131-137.
770 **Huang, B.-Q., and Russell, S.D.** (1992). Female Germ Unit: Organization, Isolation, and
771 Function **140,** 233-293.
772 **Huck, N., Moore, J.M., Federer, M., and Grossniklaus, U.** (2003). The Arabidopsis mutant
773 feronia disrupts the female gametophytic control of pollen tube reception. Development
774 **130,** 2149-2159.
775 **Huckelhoven, R., and Panstruga, R.** (2011). Cell biology of the plant-powdery mildew
776 interaction. Curr Opin Plant Biol **14,** 738-746.
777 **Iwano, M., Ngo, Q.A., Entani, T., Shiba, H., Nagai, T., Miyawaki, A., Isogai, A.,**
778 **Grossniklaus, U., and Takayama, S.** (2012). Cytoplasmic Ca2+ changes dynamically
779 during the interaction of the pollen tube with synergid cells. Development **139,** 4202-
780 4209.
781 **Johnson, M.A., Harper, J.F., and Palanivelu, R.** (2019). A Fruitful Journey: Pollen Tube
782 Navigation from Germination to Fertilization. Annu Rev Plant Biol.
783 **Jones, D.S., and Kessler, S.A.** (2017). Cell type-dependent localization of MLO proteins. Plant
784 Signal Behav **12**.

785 **Jones, D.S., Yuan, J., Smith, B.E., Willoughby, A.C., Kumimoto, E.L., and Kessler, S.A.**
786 (2017). MILDEW RESISTANCE LOCUS O Function in Pollen Tube Reception Is Linked
787 to Its Oligomerization and Subcellular Distribution. Plant Physiol **175,** 172-185.
788 **Jones, D.S., Liu, X., Willoughby, A.C., Smith, B.E., Palanivelu, R., and Kessler, S.A.** (2018).
789 Cellular distribution of secretory pathway markers in the haploid synergid cells of
790 Arabidopsis thaliana. Plant J **94,** 192-202.
791 **Kessler, S.A., and Grossniklaus, U.** (2011). She's the boss: signaling in pollen tube reception.
792 Curr Opin Plant Biol **14,** 622-627.
793 **Kessler, S.A., Shimosato-Asano, H., Keinath, N.F., Wuest, S.E., Ingram, G., Panstruga, R.,**
794 **and Grossniklaus, U.** (2010). Conserved molecular components for pollen tube
795 reception and fungal invasion. Science **330,** 968-971.
796 **Kim, M.C., Panstruga, R., Elliott, C., Muller, J., Devoto, A., Yoon, H.W., Park, H.C., Cho,**
797 **M.J., and Schulze-Lefert, P.** (2002a). Calmodulin interacts with MLO protein to regulate
798 defence against mildew in barley. Nature **416,** 447-451.
799 **Kim, M.C., Lee, S.H., Kim, J.K., Chun, H.J., Choi, M.S., Chung, W.S., Moon, B.C., Kang,**
800 **C.H., Park, C.Y., Yoo, J.H., Kang, Y.H., Koo, S.C., Koo, Y.D., Jung, J.C., Kim, S.T.,**
801 **Schulze-Lefert, P., Lee, S.Y., and Cho, M.J.** (2002b). Mlo, a modulator of plant
802 defense and cell death, is a novel calmodulin-binding protein. Isolation and
803 characterization of a rice Mlo homologue. J Biol Chem **277,** 19304-19314.
804 **Kusch, S., Pesch, L., and Panstruga, R.** (2016). Comprehensive Phylogenetic Analysis Sheds
805 Light on the Diversity and Origin of the MLO Family of Integral Membrane Proteins.
806 Genome Biol Evol **8,** 878-895.
807 **Leshem, Y., Johnson, C., and Sundaresan, V.** (2013). Pollen tube entry into the synergid cell
808 of Arabidopsis is observed at a site distinct from the filiform apparatus. Plant
809 reproduction **26,** 93-99.
810 **Leydon, A.R., Tsukamoto, T., Dunatunga, D., Qin, Y., Johnson, M.A., and Palanivelu, R.**
811 (2015). Pollen Tube Discharge Completes the Process of Synergid Degeneration That Is
812 Initiated by Pollen Tube-Synergid Interaction in Arabidopsis. Plant Physiol **169,** 485-496.
813 **Li, C., Yeh, F.L., Cheung, A.Y., Duan, Q., Kita, D., Liu, M.C., Maman, J., Luu, E.J., Wu,**
814 **B.W., Gates, L., Jalal, M., Kwong, A., Carpenter, H., and Wu, H.M.** (2015).
815 Glycosylphosphatidylinositol-anchored proteins as chaperones and co-receptors for
816 FERONIA receptor kinase signaling in Arabidopsis. Elife **4**.
817 **Lindner, H., Kessler, S.A., Müller, L.M., Shimosato-Asano, H., Boisson-Dernier, A., and**
818 **Grossniklaus, U.** (2015). TURAN and EVAN mediate pollen tube reception in
819 Arabidopsis synergids through protein glycosylation. PLoS Biol **13,** e1002139.
820 **Liu, X., Castro, C., Wang, Y., Noble, J., Ponvert, N., Bundy, M., Hoel, C., Shpak, E., and**
821 **Palanivelu, R.** (2016). The Role of LORELEI in Pollen Tube Reception at the Interface
822 of the Synergid Cell and Pollen Tube Requires the Modified Eight-Cysteine Motif and the
823 Receptor-Like Kinase FERONIA. Plant Cell **28,** 1035-1052.
824 **Mansfield, S.G., Briarty, L.G., and Erni, S.** (1991). Early embryogenesis in Arabidopsis
825 thaliana. I. The mature embryo sac. Canadian Journal of Botany **69,** 447-460.
826 **Muller, L.M., Lindner, H., Pires, N.D., Gagliardini, V., and Grossniklaus, U.** (2016). A subunit
827 of the oligosaccharyltransferase complex is required for interspecific gametophyte
828 recognition in Arabidopsis. Nat Commun **7,** 10826.
829 **Naramoto, S.** (2017). Polar transport in plants mediated by membrane transporters: focus on
830 mechanisms of polar auxin transport. Curr Opin Plant Biol **40,** 8-14.
831 **Ngo, Q.A., Vogler, H., Lituiev, D.S., Nestorova, A., and Grossniklaus, U.** (2014). A Calcium
832 Dialog Mediated by the FERONIA Signal Transduction Pathway Controls Plant Sperm
833 Delivery. Dev Cell **29,** 491-500.
834 **Okuda, S., Tsutsui, H., Shiina, K., Sprunck, S., Takeuchi, H., Yui, R., Kasahara, R.D.,**
835 **Hamamura, Y., Mizukami, A., Susaki, D., Kawano, N., Sakakibara, T., Namiki, S.,**

836 **Itoh, K., Otsuka, K., Matsuzaki, M., Nozaki, H., Kuroiwa, T., Nakano, A., Kanaoka,**
837 **M.M., Dresselhaus, T., Sasaki, N., and Higashiyama, T.** (2009). Defensin-like
838 polypeptide LUREs are pollen tube attractants secreted from synergid cells. Nature **458,**
839 357-361.
840 **Palanivelu, R., and Preuss, D.** (2006). Distinct short-range ovule signals attract or repel
841 Arabidopsis thaliana pollen tubes in vitro. BMC Plant Biol **6,** 7.
842 **Panstruga, R.** (2005). Serpentine plant MLO proteins as entry portals for powdery mildew fungi.
843 Biochem Soc Trans **33,** 389-392.
844 **Petrasek, J., Mravec, J., Bouchard, R., Blakeslee, J.J., Abas, M., Seifertova, D.,**
845 **Wisniewska, J., Tadele, Z., Kubes, M., Covanova, M., Dhonukshe, P., Skupa, P.,**
846 **Benkova, E., Perry, L., Krecek, P., Lee, O.R., Fink, G.R., Geisler, M., Murphy, A.S.,**
847 **Luschnig, C., Zazimalova, E., and Friml, J.** (2006). PIN proteins perform a rate-limiting
848 function in cellular auxin efflux. Science **312,** 914-918.
849 **Platre, M.P., Noack, L.C., Doumane, M., Bayle, V., Simon, M.L.A., Maneta-Peyret, L.,**
850 **Fouillen, L., Stanislas, T., Armengot, L., Pejchar, P., Caillaud, M.C., Potocky, M.,**
851 **Copic, A., Moreau, P., and Jaillais, Y.** (2018). A Combinatorial Lipid Code Shapes the
852 Electrostatic Landscape of Plant Endomembranes. Dev Cell **45,** 465-480 e411.
853 **Rotman, N., Rozier, F., Boavida, L., Dumas, C., Berger, F., and Faure, J.E.** (2003). Female
854 control of male gamete delivery during fertilization in Arabidopsis thaliana. Curr Biol **13,**
855 432-436.
856 **Ruge, H., Flosdorff, S., Ebersberger, I., Chigri, F., and Vothknecht, U.C.** (2016). The
857 calmodulin-like proteins AtCML4 and AtCML5 are single-pass membrane proteins
858 targeted to the endomembrane system by an N-terminal signal anchor sequence. J Exp
859 Bot **67,** 3985-3996.
860 **Salanenka, Y., Verstraeten, I., Lofke, C., Tabata, K., Naramoto, S., Glanc, M., and Friml, J.**
861 (2018). Gibberellin DELLA signaling targets the retromer complex to redirect protein
862 trafficking to the plasma membrane. Proc Natl Acad Sci U S A **115,** 3716-3721.
863 **Sandaklie-Nikolova, L., Palanivelu, R., King, E.J., Copenhaver, G.P., and Drews, G.N.**
864 (2007). Synergid cell death in Arabidopsis is triggered following direct interaction with the
865 pollen tube. Plant Physiol **144,** 1753-1762.
866 **Schindelin, J., Arganda-Carreras, I., Frise, E., Kaynig, V., Longair, M., Pietzsch, T.,**
867 **Preibisch, S., Rueden, C., Saalfeld, S., Schmid, B., Tinevez, J.Y., White, D.J.,**
868 **Hartenstein, V., Eliceiri, K., Tomancak, P., and Cardona, A.** (2012). Fiji: an open-
869 source platform for biological-image analysis. Nat Methods **9,** 676-682.
870 **Simon, M.L., Platre, M.P., Marques-Bueno, M.M., Armengot, L., Stanislas, T., Bayle, V.,**
871 **Caillaud, M.C., and Jaillais, Y.** (2016). A PtdIns(4)P-driven electrostatic field controls
872 cell membrane identity and signalling in plants. Nat Plants **2,** 16089.
873 **Sprunck, S., Rademacher, S., Vogler, F., Gheyselinck, J., Grossniklaus, U., and**
874 **Dresselhaus, T.** (2012). Egg cell-secreted EC1 triggers sperm cell activation during
875 double fertilization. Science **338,** 1093-1097.
876 **Stoorvogel, W., Strous, G.J., Geuze, H.J., Oorschot, V., and Schwartz, A.L.** (1991). Late
877 endosomes derive from early endosomes by maturation. Cell **65,** 417-427.
878 **Takeuchi, H., and Higashiyama, T.** (2016). Tip-localized receptors control pollen tube growth
879 and LURE sensing in Arabidopsis. Nature **531,** 245-248.
880 **Viotti, C., Bubeck, J., Stierhof, Y.D., Krebs, M., Langhans, M., van den Berg, W., van**
881 **Dongen, W., Richter, S., Geldner, N., Takano, J., Jurgens, G., de Vries, S.C.,**
882 **Robinson, D.G., and Schumacher, K.** (2010). Endocytic and secretory traffic in
883 Arabidopsis merge in the trans-Golgi network/early endosome, an independent and
884 highly dynamic organelle. Plant Cell **22,** 1344-1357.

885 **Wang, T., Liang, L., Xue, Y., Jia, P.F., Chen, W., Zhang, M.X., Wang, Y.C., Li, H.J., and**
886 **Yang, W.C.** (2016). A receptor heteromer mediates the male perception of female
887 attractants in plants. Nature **531,** 241-244.
888 **Yamada, M., Miyawaki, A., Saito, K., Nakajima, T., Yamamoto-Hino, M., Ryo, Y., Furuichi,**
889 **T., and Mikoshiba, K.** (1995). The calmodulin-binding domain in the mouse type 1
890 inositol 1,4,5-trisphosphate receptor. Biochem J **308 (Pt 1),** 83-88.
891 **Yang, T., and Poovaiah, B.** (2003). Calcium/calmodulin-mediated signal network in plants.
892 Trends in plant science **8,** 505-512.
893 **Yuan, J., and Kessler, S.A.** (2019). A genome-wide association study reveals a novel regulator
894 of ovule number and fertility in Arabidopsis thaliana. PLoS Genet **15,** e1007934.
895

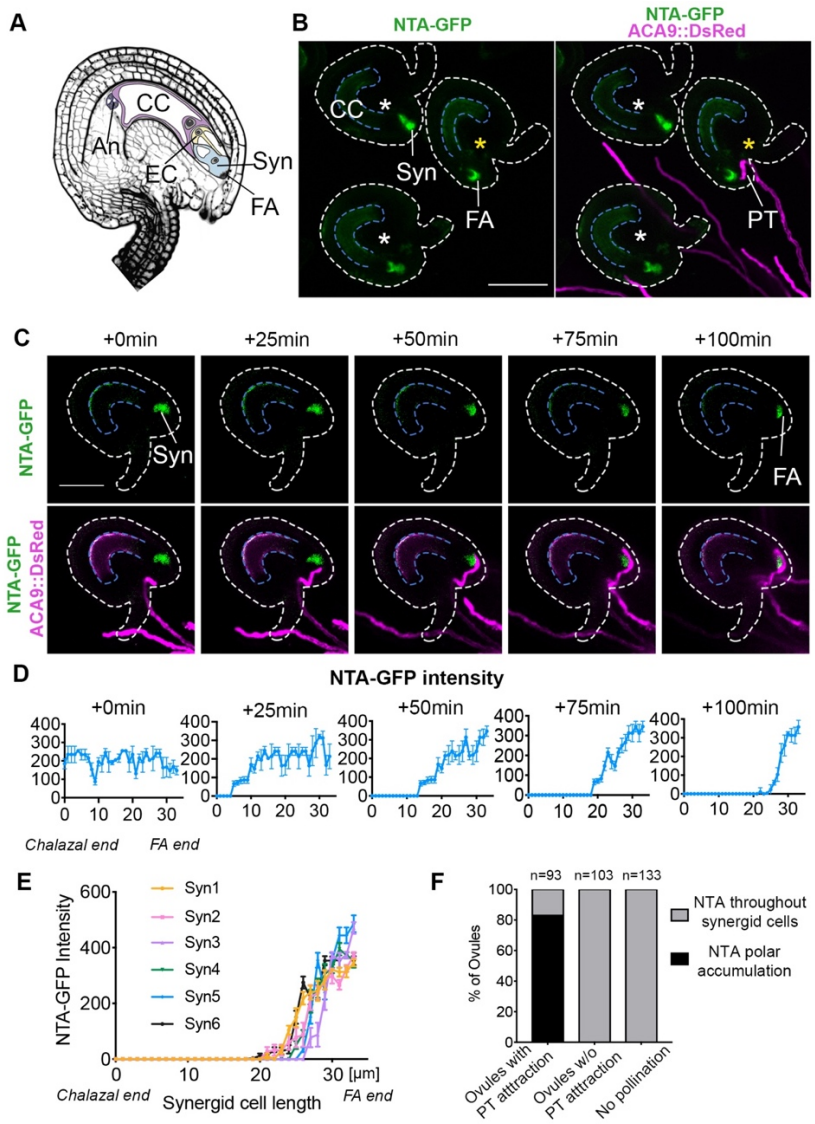

Figure 1. NTA-GFP accumulates at the filiform apparatus as the pollen tube approaches. (A) Diagram of a mature *Arabidopsis thaliana* ovule and embryo sac, modified from Jones et al, 2018. CC, Central Cell; Syn, Synergid Cells; EC, Egg Cell; An, Antipodal cells; FA, Filiform Apparatus (B, C) Live imaging of pollen tube (PT) reception using NTA-GFP labeled synergids (green signal) and ACA9::DsRed pollen tubes (magenta signal). (B) Polar NTA-GFP accumulation at the filiform apparatus (FA) occurred in ovules that attracted a pollen tube (ovules with yellow stars), while polar NTA-GFP accumulation did not occur in ovules without pollen tube attraction (ovules with white stars). (C) Time-lapse imaging of NTA-GFP accumulation during pollen tube reception. (D) Quantification of NTA-GFP signal along the length of the synergid from chalazal end (0μm) to FA end (33μm) at 0min, 25min, 50min, 75min, and 100min timepoints, respectively. (E) 6 more examples of the quantification of NTA-GFP signal along the length of synergids after pollen tube arrival. (F) Quantification of the percentage of ovules with different NTA accumulation patterns under the same imaging conditions. Bars=50 μm (B and C).

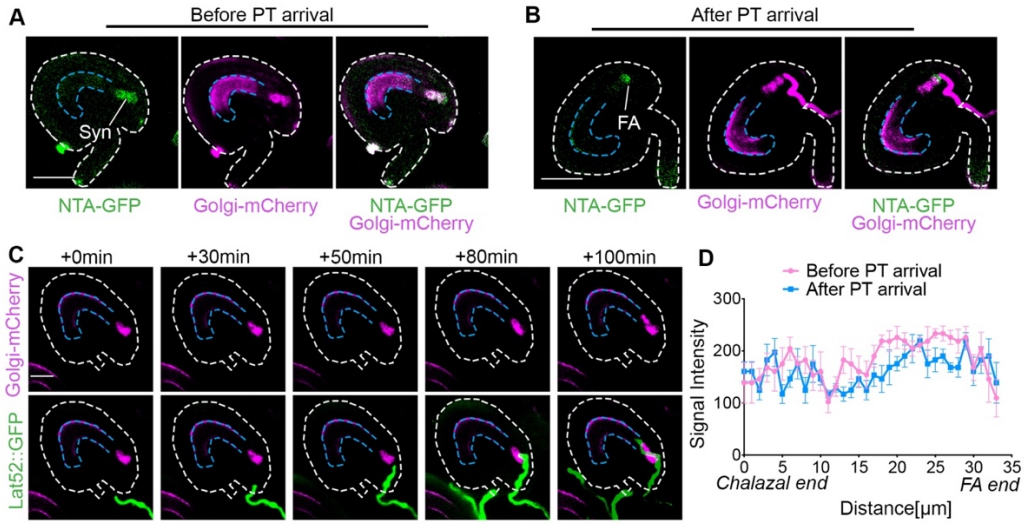

Figure 2. A Golgi marker is randomly distributed throughout synergids during pollen tube reception. (A) NTA-GFP (green signal) and Golgi-mCherry signals (magenta signal) are evenly distributed along the length of the synergid and co-localized within synergid cells before pollen tube arrival. (B) After pollen tube arrival, NTA-GFP accumulated at the FA, but Golgi-mCherry did not accumulate at the FA. (C) Live imaging of Golgi-mCherry during reception of Lat52::GFP labeled pollen tubes. (D) Quantification of Golgi-mCherry signal along the length of synergids shown in (C) before and after pollen tube arrival. Bars=30μm (A-B), 50μm (C).

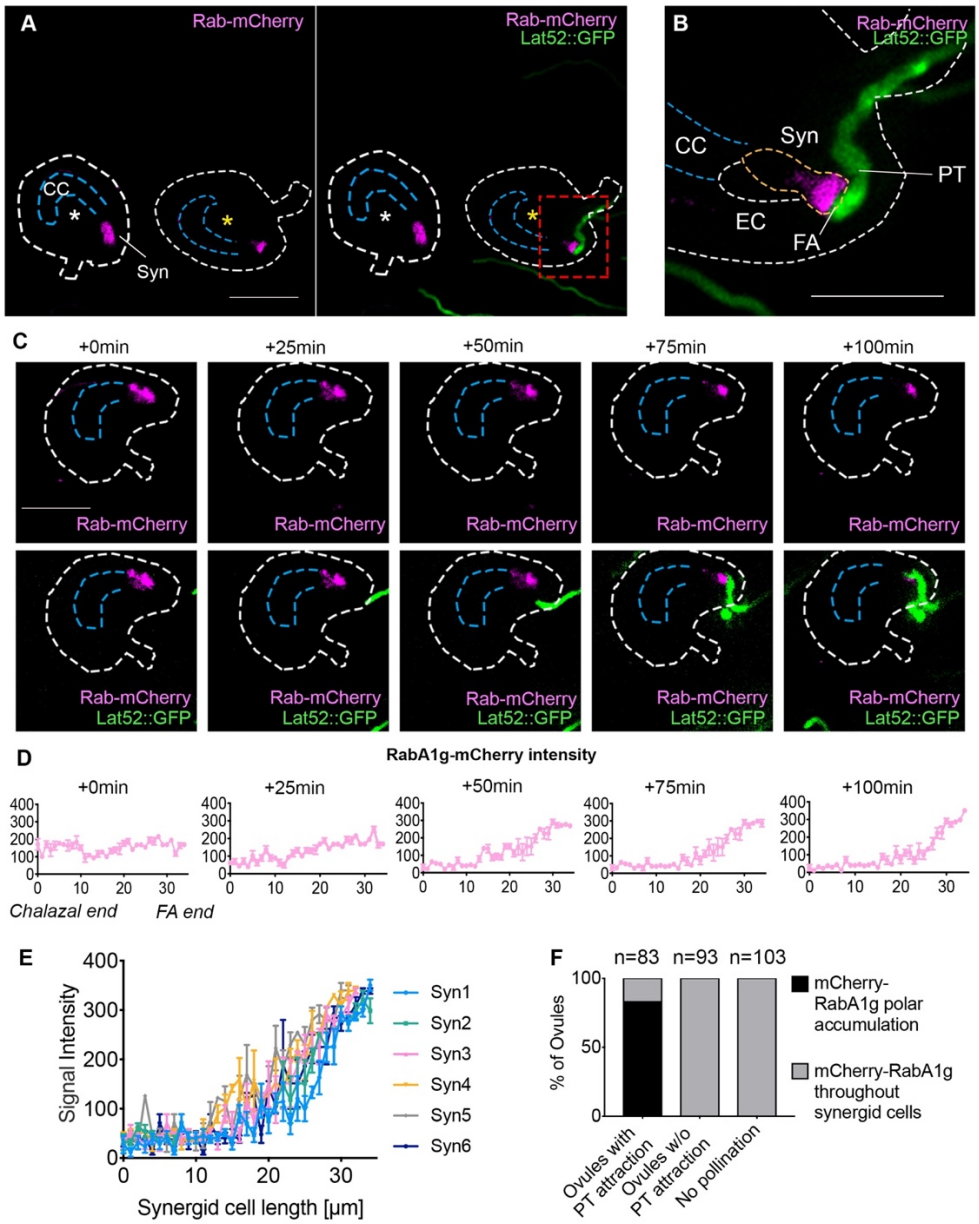

Figure 3. RabA1g endosomes polarly accumulate toward the filiform apparatus during pollen tube reception. (A) RabA1g-mCherry endosome marker (magenta signal) accumulates at the FA region in response to pollen tube arrival (ovule with yellow star). The ovule with no pollen tube attraction (white star) serves as a negative control imaged under the same conditions. (B) Higher magnification of the micropylar region of starred ovule in (red box in panel A). (C) Timing of RabA1g-mCherry polar accumulation during pollen tube arrival. Bars=50μm. (D) Quantification of RabA1g-mCherry signal along the length of synergids during pollen tube reception. Synergid cell from chalazal end to filiform apparatus (FA) end was defined from 0 to 33 μm in length. (E) 6 more examples of the quantification of RabA1g-mCherry signal after pollen tube arrival. (F) Quantification of ovule percentage with RabA1g endosome marker throughout the synergids (gray bars) or with polar accumulation at or near the filiform apparatus (black bars).

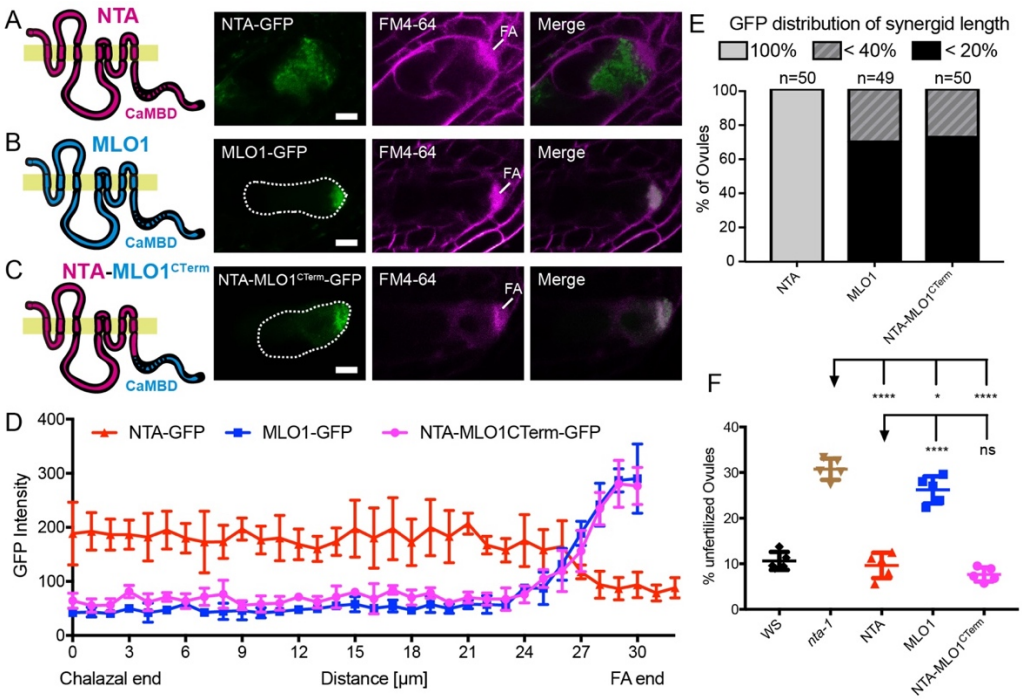

Figure 4. Targeting of NTA to the filiform apparatus before pollen tube arrival is not toxic to synergid cells. (A-C) Localization patterns of MYB98 promoter driven MLO-GFP variants (green signal) in synergids of mature virgin ovules stained with FM4-64 (magenta signal) to reveal the outline of the synergid and the filiform apparatus (FA, diffuse magenta signal). Bars = 10 µm. (D) Quantification of the GFP intensity of the MLO variants in A-C along the length of the synergids. (E) Percentage of ovules showing MLO-GFP signal throughout the synergids (100% of length), in the FA only (20% of length) and the region surrounding and including the FA (40% of length). (F) Scatter plot of unfertilized ovule percentages in homozygous plants of pMYB98::MLO-GFP in *nta-1* mutants to assess the ability of the MLO-GFP constructs to complement *nta-1*. WS, Wassilewskija. Significance was determined by a Student's *t*-test (****, $P < 0.0001$; *, $P = 0.0281$; and ns, $P = 0.2020$).

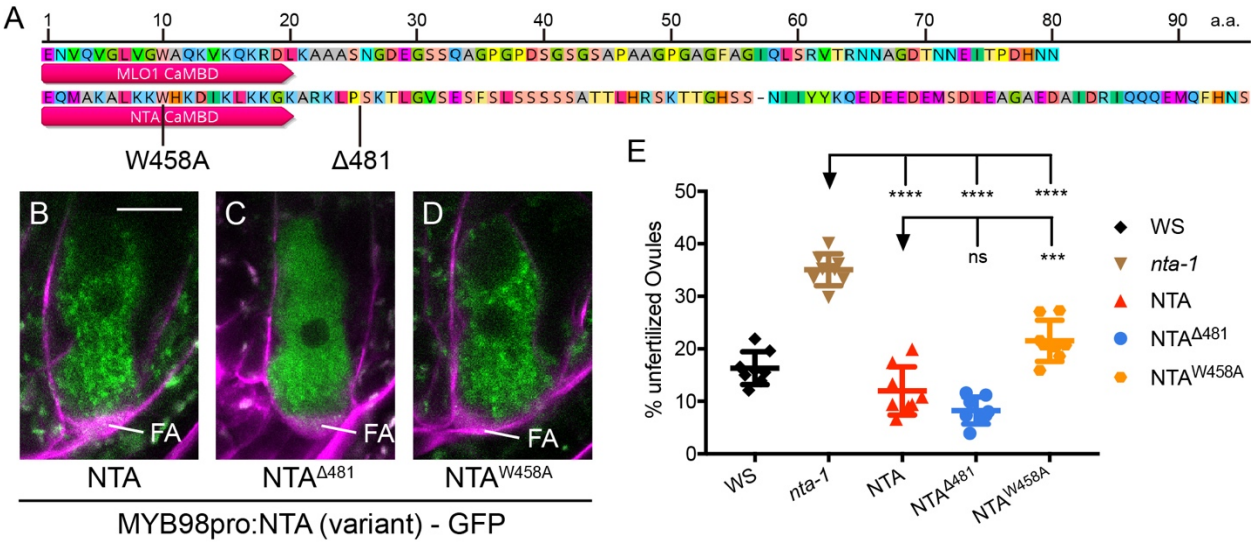

Figure 5. Disruption of the CaMBD affects NTA localization and function. (A) Alignment of MLO1 and NTA C-terminal domains after the seventh membrane span. Red bars highlight the CaMBD; W458A and Δ481 indicate the point mutation in NTA and the deletion point, respectively ; a.a., amino acid. (B-D) NTA (variant)-GFP (green) distribution in synergid cells of unfertilized ovules stained with FM4-64 (magenta signal). Bar = 10 µm. (E) Complementation analysis of NTA variants in T2 plants homozygous for $MYB98_{pro}$::NTA(variant)-GFP constructs in *nta-1* mutants. Adjusted P values from a Student's *t*-test are as follows: **** indicates $P < 0.0001$; *** indicates $P = 0.001$ to 0.0001; and ns indicates $P > 0.05$.

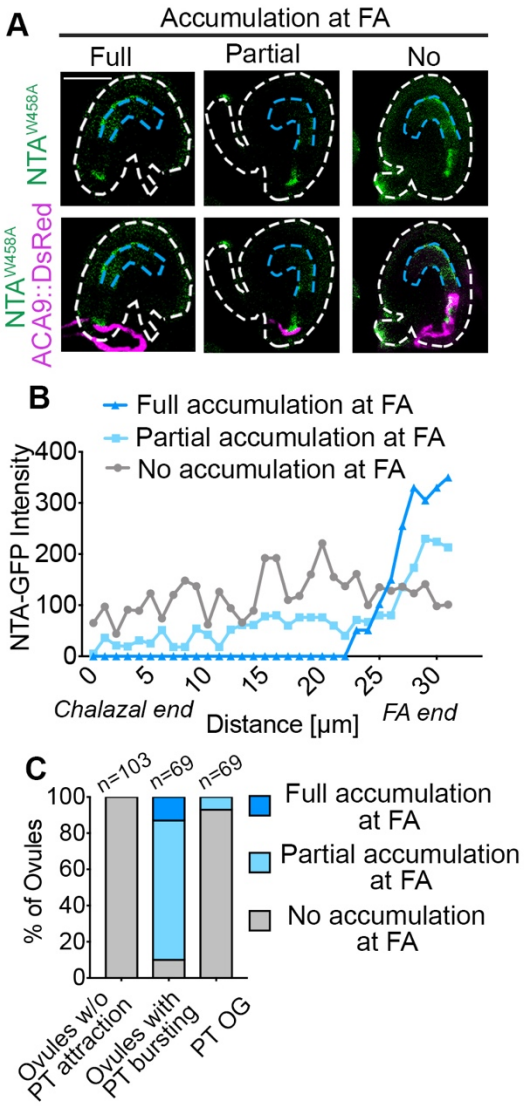

Figure 6. A point mutation in the CaMBD (NTA^{W458A}) affects filiform apparatus accumulation of NTA and pollen tube reception. (A) NTA^{W458A}-GFP has 3 different localization patterns in response to PT arrival under semi *in-vivo* conditions. Bar=50 µm (B) Quantification of GFP signal intensity in NTA^{W458A} synergids during pollen tube reception. (C) Analysis of NTA^{W458A}-GFP distribution patterns in ovules with successful (PT bursting) and unsuccessful (no PT or PT overgrowth (PT OG)) pollen tube reception.

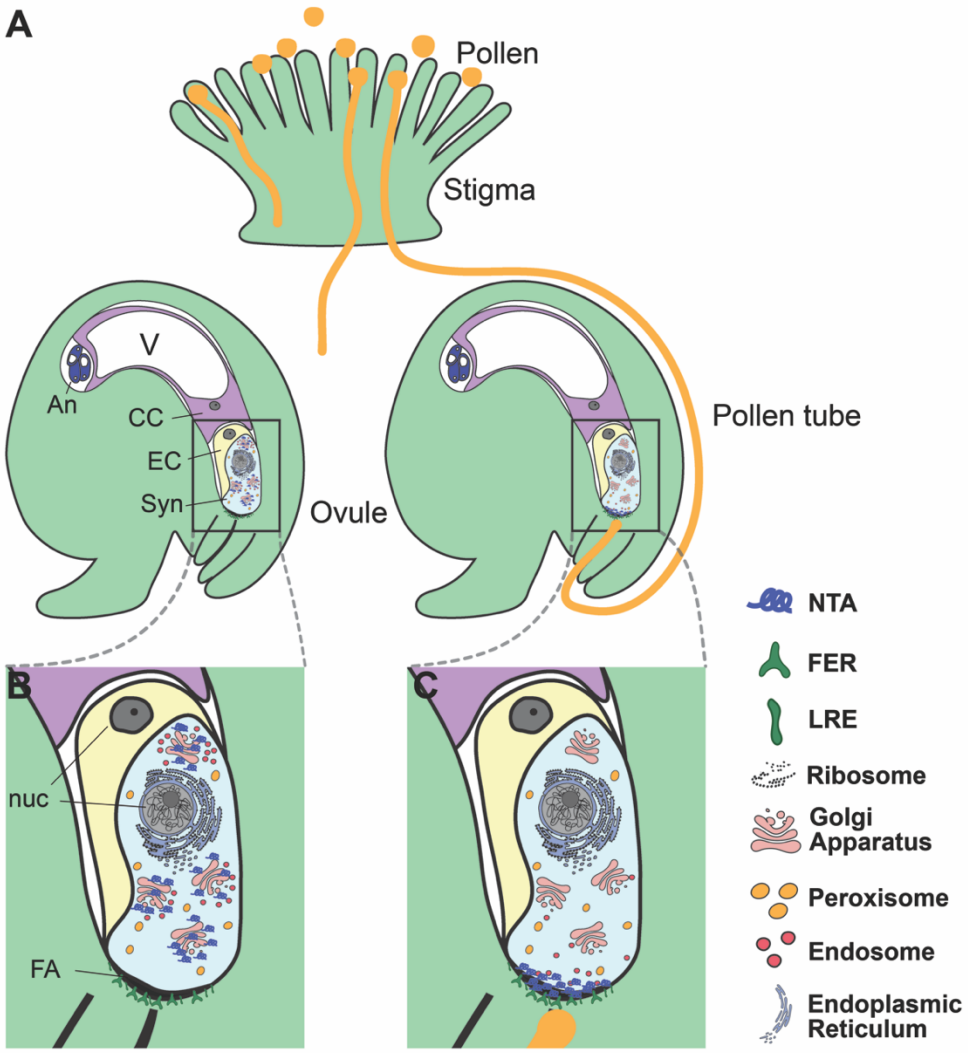

Figure 7. Subcellular dynamics in synergids during pollen tube reception. (A) Pollination using a semi-*in vivo* pollen tube guidance assay. (B) Before pollen tube arrival, NTA is in a Golgi-associated compartment and RabA1g endosomes are distributed throughout the synergids. (C) As a pollen tube arrives, NTA and RabA1g endosomes move toward the filiform apparatus (FA). NTA accumulation is dependent on signaling from the FER receptor like kinase, which acts in a complex with LRE. Abbreviations: CC, Central Cell; Syn, Synergid cells; EC, Egg Cell; An, Antipodal cells; nuc, Nucleus; FA, Filiform Apparatus.

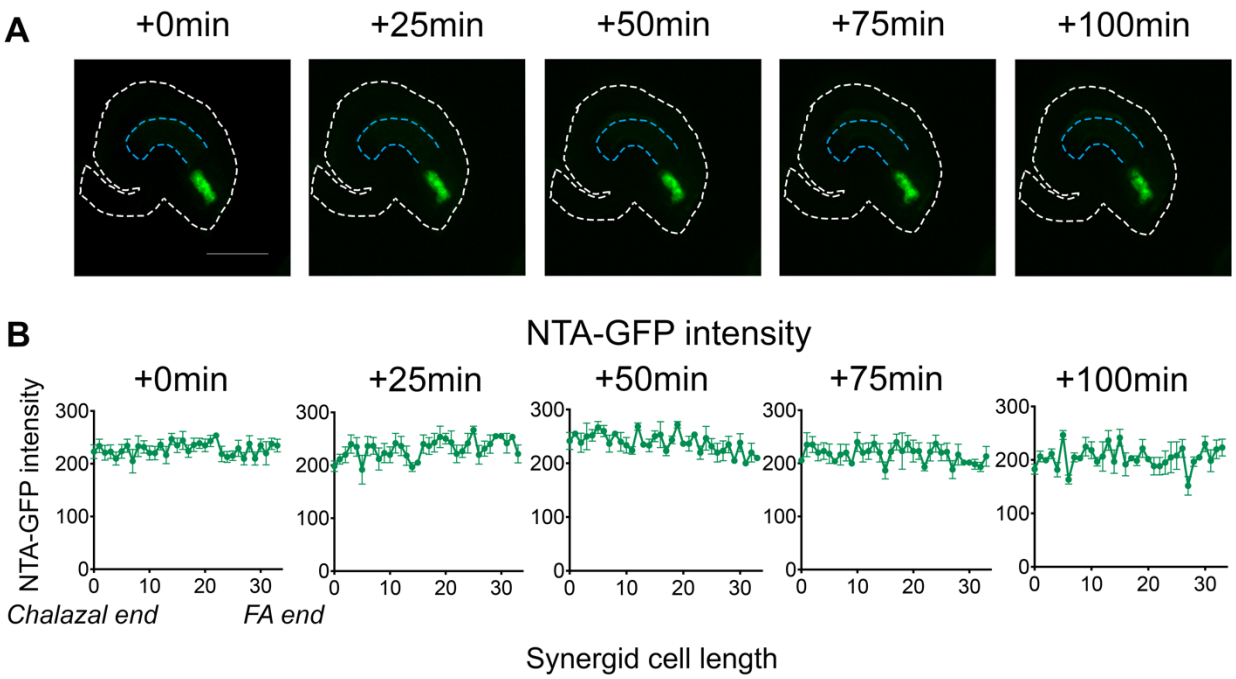

Supplementary figure 1. NTA-GFP does not polarly accumulate at the filiform apparatus in synergids without pollen tube attraction. (A) NTA-GFP (green signal) distribution pattern in synergids at 0min, 25min, 50min, 75min, and 100min timepoints, respectively. (B)Signal intensity measurement of NTA-GFP intensity at 0min, 25min, 50min, 75min, and 100min timepoints, respectively. Bar=50μm.

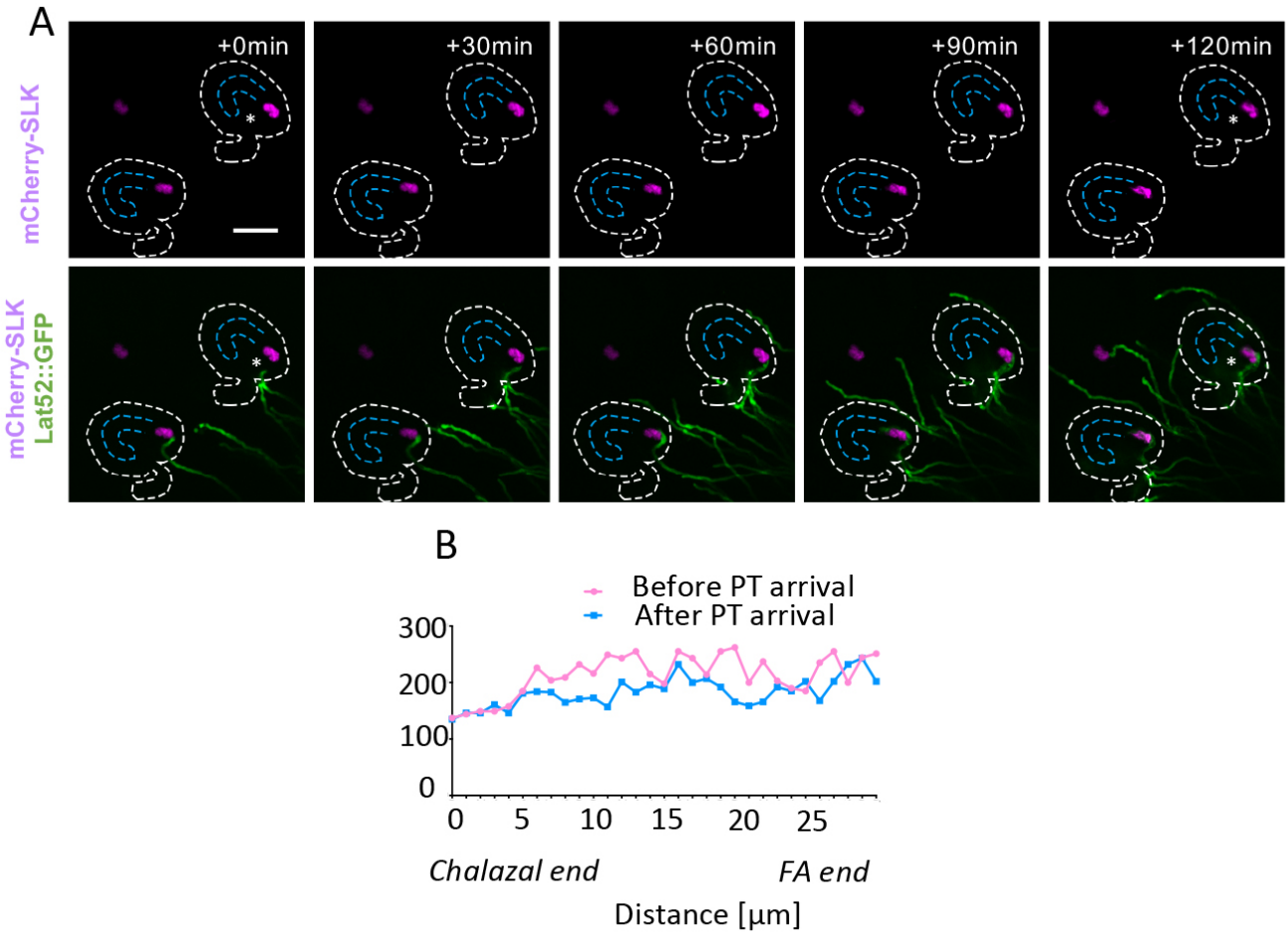

Supplementary figure 2. Peroxisomes do not exhibit polar accumulation at the FA during pollen tube reception. (A) The peroxisome marker mCherry-SLK (magenta signal) does not accumulate to the FA region after pollen tube (green signal) arrival (ovules with green stars). (B) Quantification of mCherry-SLK signal before and after PT arrival. Bars=50µm.

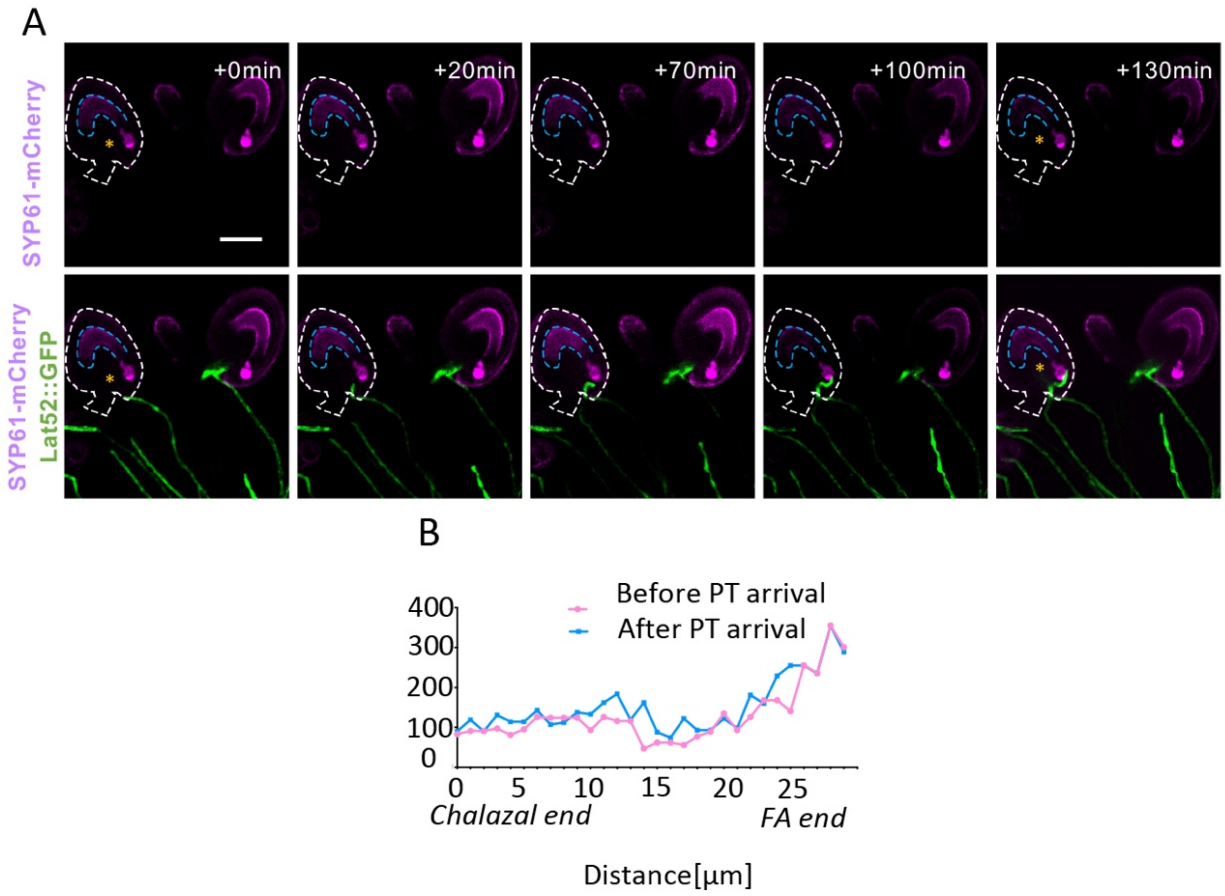

Supplementary figure 3. Trans-Golgi marker distribution in synergids does not change in response to pollen tube reception. (A) The trans-Golgi marker SYP61-mCherry (magenta signal) is concentrated toward the micropyle region of synergid cells both before and after pollen tube (green signal) arrival (ovules with yellow stars). (B) Quantification of SYP61-mCherry signal along the length of a synergid before and after pollen tube reception. Bars=50µm.

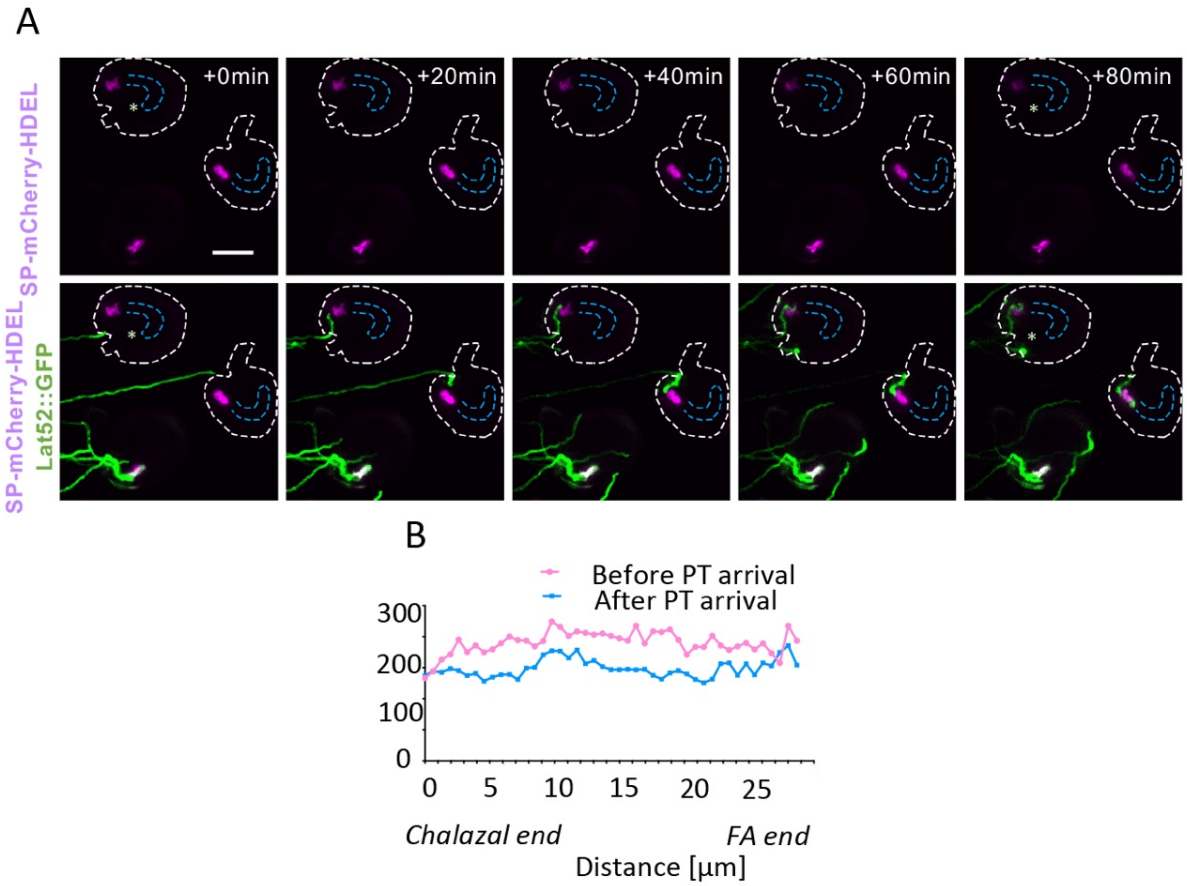

Supplementary figure 4. ER marker distribution in synergids does not change in response to pollen tube reception. (A) Before and after pollen tube (green signal) arrival, the ER marker SP-mCherry-HDEL (magenta signal) is distributed throughout synergid cells (ovules with white stars). (B) Quantification of SP-mCherry-HDEL signal along the length of synergids before and after pollen tube reception. Bars=50µm.

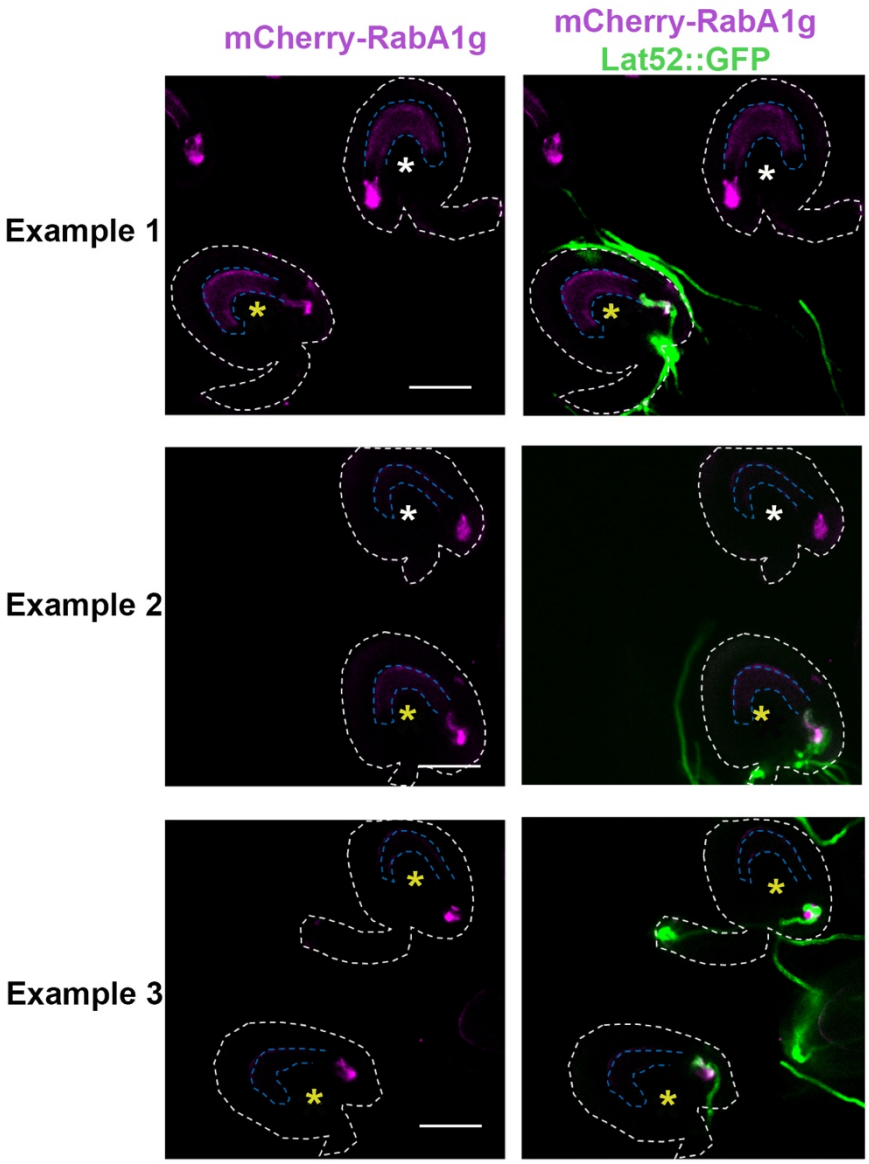

Supplementary figure 5. **Additional examples of the polar accumulation of RabA1g endosomes during pollen tube reception.** Endosome marker accumulates near the filiform apparatus region as pollen tube approaches (ovules with white stars), but no polar accumulation was found in ovules that did not attract a pollen tube (ovules with yellow stars). Bars=50μm.

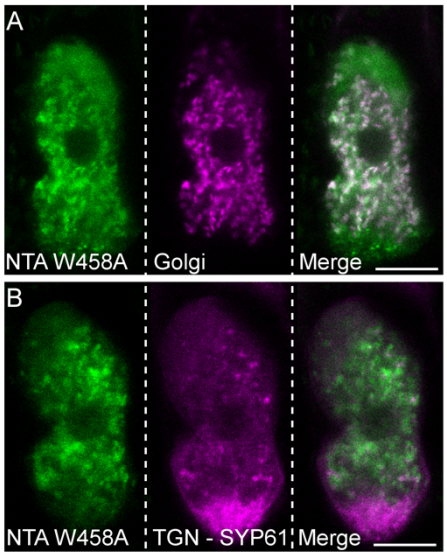

Supplementary figure 6. NTA^{W458A} co-localizes with Golgi marker in synergid cells before pollen tube arrival. Colocalization of NTA^{W458A}-GFP (green) with Golgi marker (LRE:proMan49-mCherry, magenta) (A) and the trans-Golgi network marker (TGN, MYB98pro:SYP61:mCherry, magenta) (B) in the synergid cell of unpollinated ovules. Bars = 10 μm.

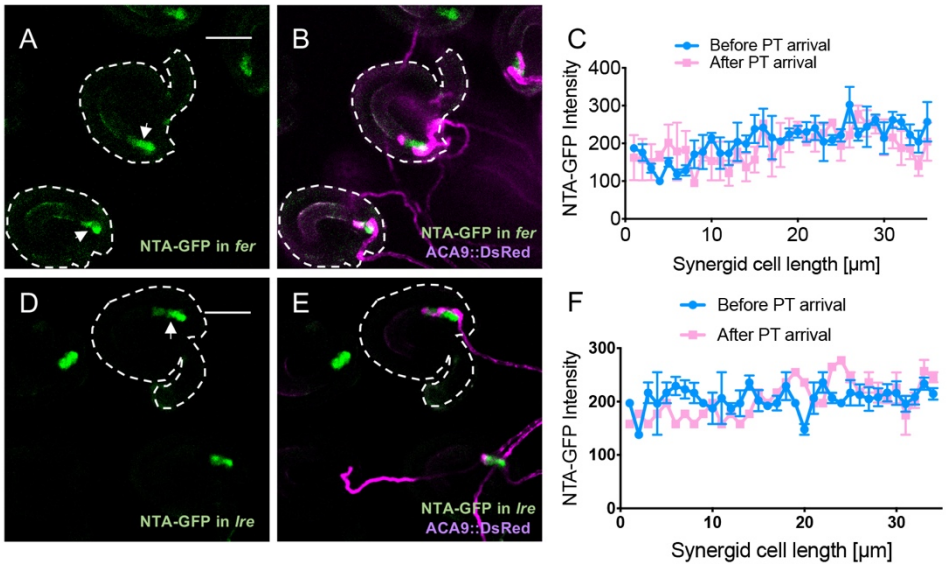

Supplementary figure 7. **NTA-GFP polar accumulation requires FER and LRE.** (A-B) In *fer* mutant synergids, NTA-GFP (green signal) distributes throughout synergids (arrows) with ACA9::DsRed pollen tube overgrowth (magenta signal). (C) Quantification of NTA-GFP signal along the length of *fer-1* synergids before and after pollen tube reception. (D-E) In *lre-7* ovules, NTA-GFP distributes throughout synergids (white arrow) with pollen tube overgrowth. (F) Quantification of NTA-GFP signal along the length of *lre-7* synergids before and after pollen tube reception. FA, Filiform Apparatus. Bars=50μm.

Supplementary table 1. List of primers used for cloning.

Primer Name	Primer Sequences (5' to 3')
NTA481-RattB2	GGGGACCACTTTGTACAAGAAAGCTGGGTGTGAAACACCAAGTGTCTTGCT
NTAW458A-F	GCATTGAAGAAG**GC**GCACAAAGACATCAAATTGAAGAAAG
NTA-RattB2	GGGGACCACTTTGTACAAGAAAGCTGGGTGAGAGTTGTGGAATTGCATCTC
NTA-FattB1	GGGGACAAGTTTGTACAAAAAAGCAGGCTTCACCATGATCACAAGAAGCAGGTGT
NTAW458A-R	C**GC**CTTCTTCAATGCCTTTGCCAT
NTA-R19	CTCATCAAACACTGCTTTCTTCATG
MLO1-F	GCAGTGTTTGATGAGAATGTGCAGGTTGGTCTTGTTG
MLO1-RattB2	GGGGACCACTTTGTACAAGAAAGCTGGGTGGTTGTTATGATCAGGTGTAATCTCA